Advanced Sensors and Sensing Systems for Structural Health Monitoring in Aerospace Composites

Raphael Olabanji Ogunleye,* Soňa Rusnáková, Jakub Javořík, Milan Žaludek, and Barbora Kotlánová

This review examines the state-of-the-art sensors and sensing technologies employed for structural health monitoring (SHM) in aerospace composites, highlighting the shift from conventional nondestructive evaluation techniques to real-time monitoring systems. The review discusses the challenges associated with composite materials, such as their anisotropic nature and susceptibility to invisible damage, and how these challenges have driven the improvement of SHM techniques. Fiber-optic sensors, including interferometric, distributed, and grating-based sensors, are analyzed for their high sensitivity and multiplexing capabilities, making them suitable for distributed sensing applications. Piezoelectric sensors are evaluated for their effectiveness in both active and passive damage detection methods. At the same time, piezoresistive self-sensing systems are explored for their potential to integrate sensing directly into composite materials. The review also addresses the challenges encountered in implementing SHM systems. It suggests solutions like protective coatings, advanced data processing algorithms, and modular system design to overcome these challenges. In conclusion, this review provides a comprehensive overview of the current SHM technologies for aerospace composites, underscoring the need for sustained research and development to improve sensor technology, expand data processing capabilities, and ensure seamless integration with aircraft systems, thus contributing to the safety and efficiency of aerospace operations.

1. Introduction

The advent of advanced composite materials marks a transformative phase in aerospace engineering, profoundly changing the approach to aircraft design and manufacturing.[1] Traditionally, aircraft have relied heavily on metals such as aluminum and titanium for their strength, durability, and weight properties. However, the limitations of these conventional materials, such as sensitivity to corrosion, fatigue, and sheer weight, have prompted the aerospace industry to explore alternative solutions.[2] Advanced composite materials, such as carbon fiber-reinforced polymers (CFRPs) and glass fiber-reinforced polymers (GFRPs), offer significant advantages over their metal counterparts.[3] These composites boast superior strength-to-weight ratios, enhanced fatigue resistance, and greater design flexibility.[4] As a result, they have rapidly become integral to modern aircraft, contributing to improved fuel efficiency, reduced emissions, and more incredible overall performance.[5] This shift toward composite materials is not just an incremental improvement but a revolution in aviation, driving innovation and shaping the future of flight. A prime example of this revolution is the Boeing 787 Dreamliner, where ≈50% of the primary structure, including the fuselage and wings, is constructed from CFRP (**Figure 1**).[6] This extensive use of composites results in a lighter aircraft, achieving up to 20% better fuel economy compared to traditional aluminum designs.[1]

Despite their numerous advantages, advanced composites are not without their challenges. One significant vulnerability lies in their laminated structure, with relatively low out-of-plane properties compared to their high in-plane strength and stiffness.[7] Hence, failures such as matrix cracking and delamination significantly limit their usage. Furthermore, predicting damage in composites is challenging due to their anisotropic nature.[8] Factors such as material composition, environmental conditions, and the type and direction of stress applied can also significantly impact how composites fail, making it intricate to anticipate the exact type of failure.[9]

Moreover, composite damage might be invisible, especially in aerospace, where impact damage due to lightning strikes and other environmental conditions could compromise the internal integrity of the structure.[10] Consequently, detecting various failure modes in the structure during usage and continuous health monitoring throughout their service life has become increasingly vital and indispensable. As a result of the paramount emphasis on safety and reliability, structures for aerospace applications are

R. O. Ogunleye, S. Rusnáková, J. Javořík, M. Žaludek, B. Kotlánová
Department of Production Engineering
Faculty of Technology
Tomas Bata University in Zlín
Vavrečkova 5669, 76001 Zlín, Czech Republic
E-mail: ogunleye@utb.cz

The ORCID identification number(s) for the author(s) of this article can be found under https://doi.org/10.1002/adem.202401745.

**ADVANCED
SCIENCE NEWS**

www.advancedsciencenews.com

**ADVANCED
ENGINEERING
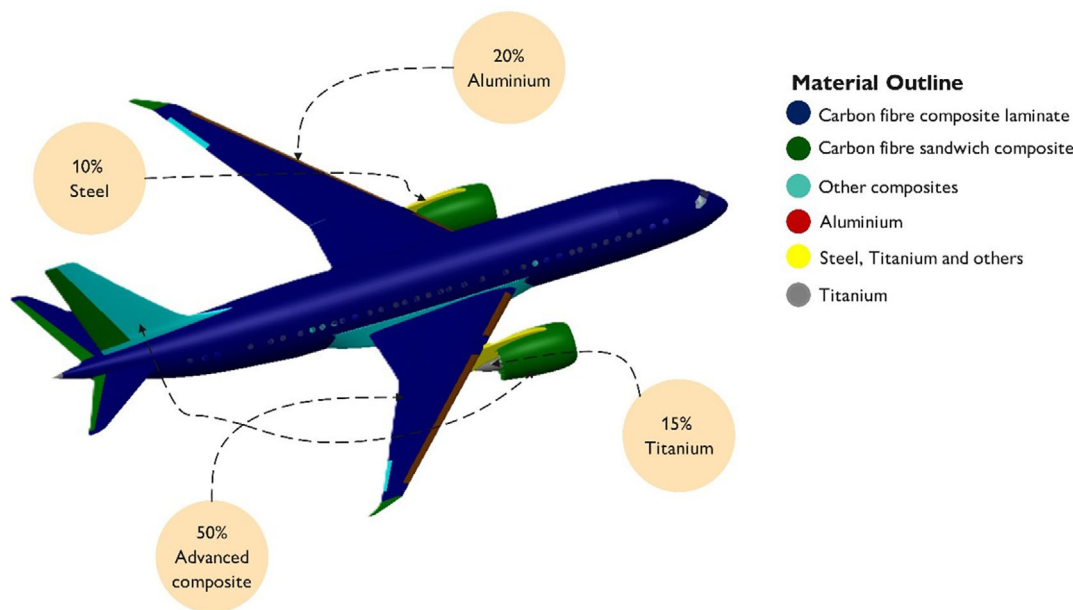MATERIALS**

www.aem-journal.com

Figure 1. Distribution of material in Boeing 787 aircraft.

often overdesigned.[11] This approach involves incorporating additional material and structural reinforcements beyond the calculated requirements, ensuring a substantial safety margin. Overdesigning provides a buffer against uncertainties, but it also comes with certain drawbacks, such as increasing the weight of the aircraft, thus impacting the overall performance and fuel efficiency.[12]

One promising approach to harnessing the full potential of advanced composite material for aerospace applications is to develop the capability to detect and continuously monitor its internal damage state.[13] This process enables the establishment of appropriate safety precautions, thereby mitigating the risk of failures. Structural health monitoring (SHM) is a technique utilized to assess the condition and performance of structures in real-time.[14] The primary objective of SHM is to ensure the safety, reliability, and longevity of these structures.[15] It involves using various nondestructive techniques, sensors, and other monitoring devices to collect data and analyze structural behavior and integrity.[16] Research on damage and failure analysis of composite has significantly increased in recent years due to the increasing application of the material in the aerospace industry, coupled with advancements in sensor and sensing technologies and a greater emphasis on data-driven approaches in modern industries.[17] A sensing system in a composite structure allows critical parameters such as strain, temperature changes, and vibration levels to be continuously monitored in real-time.[16,17] Hence, this review discusses different types of sensors and sensing approaches for effective SHM of aerospace composite structures.

2. Nondestructive Evaluation of Aerospace Structure

Nondestructive evaluation (NDE) can be described as the examination of a structural material without damage or negatively

affecting its usage.[18] Depending on the industry and area of application, NDE is also widely referred to as nondestructive testing (NDT) or nondestructive inspection (NDI). The difference is that NDT focuses on the testing aspect by emphasizing the procedure utilized in testing the structure without resulting in damage.[19] In contrast, NDI focuses on the inspection and monitoring of the structure to ensure safety and reliability.[20] Irrespective of the competency, the specific objective of NDE is to ensure reliability, prevent accidents, and save lives.

In the aerospace industry, NDE is utilized during production and in-service use (**Table 1** and **2**).[21] The application of NDE for these two core areas has evolved over the years due to the evolution of structural materials from cloth biplanes to metallic structures to advanced composite materials (**Figure 2**). The emergence of the NDE for aerospace applications can be traced back to the early 19th century, prior to the establishment of the Wright Company by the Wright brothers (Orville and Wilbur Wright) in 1909 and the Boeing Airplane Company by William Boeing in 1916.[22] Visual inspection is one of the earliest and most fundamental NDEs.[23] It was particularly crucial in the early days of aviation, such as with cloth-biplane aircraft. During the manufacturing process of these aircraft, visual inspection played a crucial role in the identification of damages such as cloth wear, wood frame bending, and adhesive failure.[24]

Advancements in aircraft structures, from cloth and wood to aluminum, led to the introduction of radiographic and magnetic particle inspection (MPI).[25] Radiographic inspection relies on a radiation source (film X-ray) that passes through the structure to identify voids, cracks, and even moisture in the metallic core commonly used for the flight control surface. These defects usually absorb less radiation, creating differences in the intensity of the radiation that reaches the detector.[26] Modern X-ray radiography, such as digital radiography (DR) and X-ray computed tomography, has the advantage of providing a digital set, minimizing cost, and eliminating the environmental effect and, thus,

Table 1. NDE for examination of aerospace structural components.

Technique	Principle	Advantages	Limitation
Visual inspection[195]	It involves visualizing a component or structure, sometimes with optical aids that provide a magnified view or access to hard-reach areas.	(a) Requires relatively inexpensive tools and minimal setup; (b) it provides instant feedback on the condition of the structure.	(a) Internal defects cannot be identified; (b) accuracy of the inspection depends on the skills and experience of the inspector; (c) it is time-consuming; (d) complex geometry parts are challenging to inspect.
Penetrant testing[196]	The technique is utilized to detect surface defects in nonporous parts through the application of a penetrant liquid on the structure surface. Then, a blotter (developer) is applied to draw the penetrant out of the defects, thereby creating a visible defect profile on the surface.	(a) Fine surface-breaking defects are detectable; (b) suitable for both metallic and composite structures; (c) relatively low cost and simple process	(a) It cannot detect internal defects, (b) it is time-consuming, (c) it is sensitive to environmental conditions such as temperature and lighting, and (d) it involves handling chemicals that require proper disposal and safety measures.
Film X-ray radiography[197]	Film X-ray radiography involves passing X-rays through an aircraft component and capturing the image on a photographic film. The film is then developed using chemical processes to create a radiographic image that reveals possible defects in the structure.	(a) Captures fine details, which are helpful in identifying small cracks and corrosion pits. (b) Efficient in detecting moisture in the metallic core. (c) The accuracy of the analysis depends on the skills and experience of the inspector	(a) Chemical development is required, which is time-consuming and involves hazardous materials. (b) Physical storage space for the films is required and may degrade with time
X-ray computed radiography[197]	It is similar to film radiography, but the emitted X-rays are captured by a digital detector instead of the film. Image data are recorded and processed by the computer to detect structural defects.	(a) Faster processing as it eliminates chemical development. (b) Images are stored electronically, facilitating easy access, sharing, and archiving. (c) Digital images can be improved and manipulated for better defect detection and analysis. (d) Reduces environmental impact by avoiding chemical use	(a) It requires an expert to use and interpret digital images effectively. (b) Lower resolution compared to high-quality film

Table 2. NDE for examination of aerospace structural components (continuation).

| Technique	Principle	Advantages	Limitation
MPI[28]	The structure or components to be inspected are magnetized using a magnetic field, either by direct magnetization (current passing through the component) or indirect magnetization (external magnetic field). The applied magnetic field induces magnetic field lines within the structure. Any surface or near-surface defects, such as cracks or voids, disrupt the magnetic field lines.	(a) Highly effective for surface and near-surface defect detection. (b) Provides immediate visual indications of defects. (c) Portable equipment allows for in-service inspections	(a) Near-surface defects only. (b) Limited to ferromagnetic structure.
ECT[198]	An AC is passed through a coil, generating a time-varying magnetic field. When the coil is placed near a conductive component, the changing magnetic field induces circulating currents, called eddy currents, in the material. Any discontinuities, such as cracks or corrosion, disrupt the flow of eddy currents, causing changes in their distribution and characteristics.	(a) Applicable to a wide range of conductive materials, including metals used in aircraft structures. (b) Effective for inspecting complex shapes and geometries. (c) Noninvasive	(a) Depth limitation. (b) Conductive materials only. (c) Highly skilled expertise is required.
Magneto-optical imaging[199]	It combines magnetic field detection with optical imaging to leverage the magneto-optical effect in visualizing magnetic field variation that indicates structural defects.	(a) High sensitivity to surface and near-surface defects. (b) High-resolution image with detailed information on the flaws. (c) Possibility for in-service use. (d) Noninvasive	(a) Limited to ferromagnetic component. (b) Limited depth. (c) Highly skilled expertise is required
UT[29]	UT utilizes high-frequency stress waves produced at the surface to interrogate the structure for flaws that reflect or attenuate the signal.	(a) It can detect internal defects deep within the structure. (b) It is susceptible to minor defects and provides high-resolution imaging. (c) Suitable for both electrically conductive and nonconductive material. (d) Capability to identify in-service damages	(a) Highly skilled expertise is required. (b) It depends on the use of a couplant for effective wave transmission. (c) It is challenging to inspect complex geometries and irregular shapes
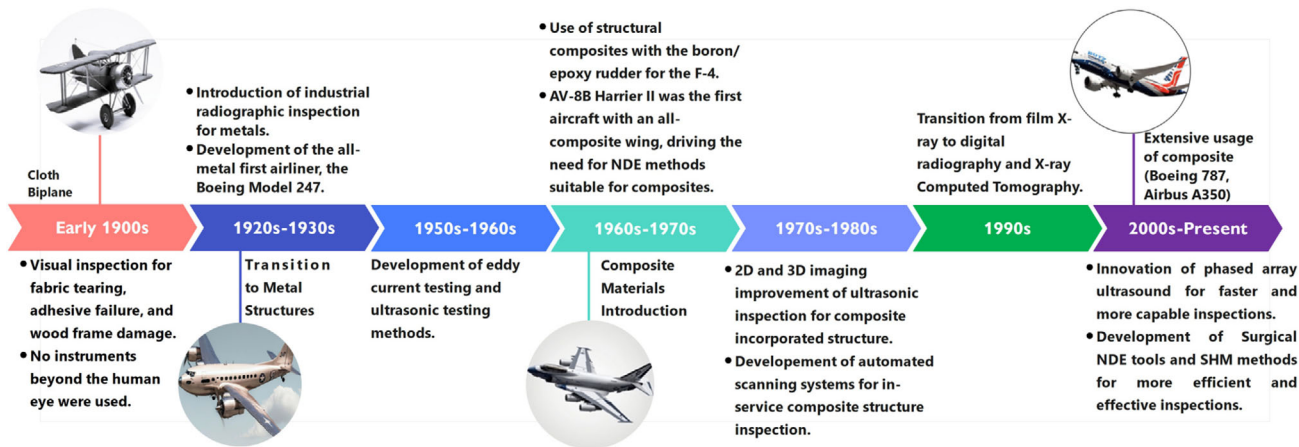
Figure 2. Trends in NDE technology for aerospace structural applications.

has replaced the film X-ray.[27] Likewise, MPI relies on a magnetic field that induces a magnetic flux line to the structure. Any instances of discontinuity in the flux line indicate the presence of defects in the structure.[28]

Furthermore, the emergence of the first eddy current testing (ECT)[29] and ultrasonic testing (UT) technique[29] revolutionized the NDE approach, reducing inspection challenges and opening opportunities for advanced low-frequency testing of the aircraft structure. Unlike the MPI, which uses magnetic fields and ferromagnetic particles to detect cracks, ECT utilizes electromagnetic induction to generate an alternating magnetic field that induces eddy currents in the conductive aircraft structure. Changes in material properties, such as cracks or corrosion, affect the eddy currents, which in turn change the impedance of the coil. Advances in ECT technology led to the development of magneto-optical scanning that allows two-dimensional eddy current-based imaging of cracks in some complex parts, such as in the fastener region and fuselage lap joint.[30] UT relies on the principle of sound wave propagation through a material. A transducer generates ultrasonic waves, which travel through the material. When these waves encounter a boundary between different materials or a defect within the material, part of the energy is reflected to the transducer. Hence, the defect's presence, size, and location can be identified by analyzing the time the sound waves travel and the amplitude of the reflected signals.[31] UT has the advantage of the ability to discover more profound defects than ECT and can also be utilized for a nonelectrically conductive structure.

The use of advanced composite materials in the manufacturing of aircraft structures has considerably increased since Boeing developed the F-4 aircraft with a rudder made from boron/epoxy in the 1960s.[32] Today, aircraft such as the Boeing 787 are manufactured with over 50% of their weight and 60% of their volume comprised of composite materials.[6] Many aircraft manufacturers (Airbus, Bombardier, Embraer, and Dassault Aviation) are now adopting composite materials for their parts instead of metal due to several advantages.[33] Unlike metal, composites support the creation of larger, more integrated designs. They can be engineered to have specific properties, such as enhanced stiffness or tensile strength.[32]

Additionally, composites are resistant to fatigue and corrosion, which translates to lower maintenance costs and fewer required inspections.[9] However, the complexity of composite structures led to innovation in NDE.[34] Traditional inspection methods are not sufficient to identify issues like delamination, voids, or fiber breakage within composites.[35] Also, traditional NDE approaches like ECT and MPI are only suitable for metallic structures.[36] This limitation further underscores the innovative NDE methods specifically designed for composite materials. Advanced techniques such as UT and DR are developed and refined to inspect composite parts.[37] UT has significantly advanced, enabling 2D and 3D imaging and sophisticated data analysis capabilities. These improvements have been particularly beneficial for inspecting composite structures, where traditional methods may not suffice due to their complex internal geometries and material variations. Automated UT scanning devices have been developed specifically for both production and in-service inspection of composite structures.[38] These devices are designed to precisely map internal defects such as delamination, voids, and fiber breaks. They automate the scanning process, ensuring thorough and consistent inspections while reducing dependency on operator skills.

While many of these NDEs are still being utilized for structural damage testing. However, as the aerospace industry advances, especially in the application of advanced composite for structural components, it becomes indispensable to ensure that aircraft structures are free from multiple site damage, which can interact and coalesce, leading to rapid crack propagation and potentially catastrophic failure.[39] Thus, it is essential to develop a new monitoring approach, such as the SHM. The SHM involves the continuous, autonomous, and in-service assessment of structural integrity, environmental conditions, and flight parameters. This is achieved by permanently attaching or embedding a network of advanced sensors within the aircraft structure.[13] These sensors continuously collect and transmit data on various aspects of the aircraft's condition, allowing for real-time monitoring and early detection of potential issues. Unlike the NDE technique, in which structural integrity is routinely observed, SHM sensors are permanently installed on the aircraft structure. Thus, inspection intervals are drastically

reduced, and minor damage can be detected with an immediate repair strategy.[40]

The SHM technique significantly enhances inspection efficiency by minimizing test interruptions and reducing human error. It allows for the simultaneous and instant monitoring of a wide area of the structure, including hidden and inaccessible regions. This comprehensive coverage drastically reduces inspection time and improves the overall reliability of the structural assessment.[41]

Regarding the monitoring of advanced aerospace composite structures, SHM can continuously monitor these materials, helping to detect impact, delamination, fiber debonding, and water ingress with their respective localization, intensities, and sizes early.

3. Sensors for Structural Health Monitoring of Aerospace Composite Structure

Generally, sensors for SHM systems need to meet specific requirements to ensure accurate, reliable, and efficient monitoring. First, the sensor must be sensitive to detect subtle changes and reliably transmit acquired information without frequent calibration or maintenance.[42] Second, structures for aerospace applications are often subjected to harsh environmental conditions, including extreme temperature, vibration, and high humidity.[43] Hence, the sensor must be durable and capable of withstanding these conditions without degradation in performance. Third, nonintrusive sensors are preferred for compatibility considerations to avoid altering or compromising the mechanical properties of the composite. Also, sensors with fast response time to capture dynamic events are essential for real-time monitoring and early warning systems.[44] Finally, a sensor for SHM of aerospace structures should be relatively small, have low density and power consumption, have high resistance to electromagnetic interference, and be cost-effective to allow for widespread adoption.[45]

Several studies on SHM of composite have reported the usage of sensors installed either by embedding or mounted on the surface of the composite structure with the purpose of SHM during the production and in-service monitoring operation.[46–48] While SHM techniques are novel, some promising sensors capable of being adopted for aerospace applications are discussed below.

3.1. Fiber-Optic Sensors

The emergence of fiber-optic sensors as vital tools for SHM can be attributed to their unparalleled sensitivity and remarkable multiplexing capability.[49] Sensitivity signifies the sensors' ability to detect microscopic changes in the environment they monitor, such as subtle shifts in strain, temperature, pressure, or vibrations within structures.[50] This high sensitivity allows them to identify early signs of structural degradation or potential failures, enabling timely intervention and maintenance.

Furthermore, the multiplexing capability of some fiber-optic sensors enhances their utility significantly. Multiplexing is the simultaneous use of multiple sensors within a single optical fiber cable.[16] Unlike conventional sensors, which often require individual wiring for each measurement point, fiber-optic sensors can be interconnected along a narrow single cable. This feature enables monitoring numerous parameters at various locations within a structure using a streamlined and efficient system. Consequently, it reduces the complexity of the monitoring setup, minimizes installation costs, and simplifies the overall data collection process.[51]

Fiber-optic sensor technology has evolved since its early applications in the 1980s. Some of these innovations have transitioned into the commercial market, becoming readily accessible for various applications.[52] These sensors encompass various functionalities, including measuring parameters like strain, temperature, pressure, and vibration. Based on their application for SHM, fiber-optic sensors can be categorized into interferometric sensors, distributed sensors, and grating-based sensors.

3.1.1. Interferometric Fiber-Optic Sensors (IFOS)

IFOS exploit interference patterns created by multiple reflections of light between two parallel surfaces.[53] They consist of an optical fiber with a cavity formed by two reflective surfaces. The cavity can be formed by the end-face of the fiber and a separate reflecting surface or two reflecting surfaces within the fiber itself. The surfaces are designed to transmit partially and reflect light, thus creating interference patterns.[54] Therefore, when the composite structure undergoes strain, the mechanical deformation affects the length of the cavity. This change in length alters the interference pattern, causing a shift in the reflected light spectrum, which can be correlated with the magnitude of strain.[55] Fabry-Perot interferometric sensor (FPI) is the most common interferometric sensor possessing a relatively high strain resolution with a magnitude of $0.15\,\mu\varepsilon$ and a capacity of measuring strain up to $\pm500\,\mu\varepsilon$ within an operating temperature of -40 to $1000\,°C$, making them versatile for monitoring structural changes under extreme environmental conditions.[56]

FPI sensors are classified into intrinsic FPI (IFPI) and extrinsic FPI (EFPI) (**Figure 3**). The difference is that for IFPI fabrication, the cavity is typically formed directly within the core of an optical fiber by introducing reflectors (mirrors) at specific points along the fiber.[57] However, a cavity is developed in EFPI by incorporating a separate interferometer into the optical path, usually by placing a small, reflective diaphragm or mirror at the end of a fiber.[58]

Although IFPI sensors are minimally invasive and introduce very little disturbance to the material (particularly important in aerospace applications where material integrity is critical), they can still present challenges.[59] One key issue is the potential coupling with transverse strain.[60] In composite materials, strain often occurs in multiple directions due to their anisotropic nature. While IFPI sensors are designed to measure longitudinal strain, they can also be affected by transverse strains. This cross-sensitivity means that the sensor might register changes not only from the intended longitudinal strain but also from unintended transverse strains. Misinterpreting the strain data due to transverse strain coupling can lead to false positives (indicating damage where there is none) or false negatives (failing to detect actual damage).

In contrast to IFPI sensors, EFPI sensors, as shown in Figure 3b, are characterized by a unique configuration that
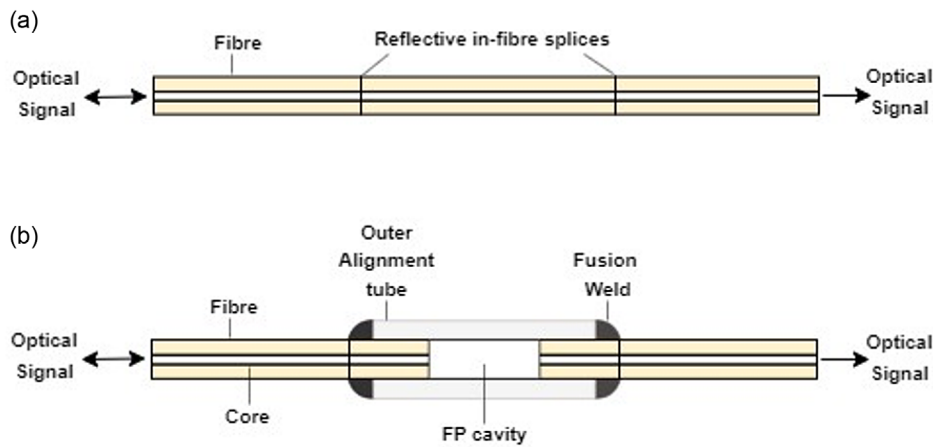
Figure 3. Types of FPI: a) IFPI b) EFPI.

includes a pair of optical fibers encased within a hollow glass cylinder. These fibers are typically joined to the tube through either fusion splicing or adhesive bonding techniques.[61] The length of the glass tube typically varies between 0.003 and 0.04 m, with an external diameter that can reach up to 0.3 mm, making it slightly wider than the optical fibers themselves. The ends of the optical fibers are mirrored and oriented at right angles to the longitudinal axis of the fiber, and they are separated by a cavity filled with air. One of the fibers acts as the input/output channel for the light signal, while the other fiber is used to reflect the signal, creating the interferometric effect. An EFPI sensor determines free strain in composite by detecting variations in the length of the air gap between the two optical fibers, which correspond to a phase shift in the light signal between the input/output fiber and the reflective fiber. The optical fibers within the EFPI sensor can be configured as single-mode, multimode, or a hybrid of the two to suit specific application requirements.[62] The sensitivity of the EFPI sensor can be enhanced by applying metal or dielectric coatings to the mirrored ends of the fibers, which optimizes the reflectivity and, consequently, the precision of the strain measurements.

The benefits of using EFPI sensors for strain damage monitoring for the aerospace composite are multifaceted. Aerospace structures are subject to complex stress states that include both axial and transverse strains. EFPI sensors' ability to remain unaffected by transverse strain allows for more accurate measurement of the axial strain component, which is critical for assessing the structural integrity of aircraft components under various loading conditions.[62] This specificity ensures that the data collected by the sensors accurately reflects the primary strain of interest, thereby enhancing the reliability of structural health monitoring systems. Likewise, aircraft operate in environments with wide temperature variations, from the extreme cold of high-altitude flight to the heat of re-entry or ground operations in hot climates. The fact that EFPI sensors are not sensitive to transverse temperature changes means that they can provide consistent strain measurements regardless of the ambient temperature.[61] Also, the robustness of EFPI sensors, as indicated by their high failure strain of up to 1.2%, is particularly advantageous for aerospace applications where materials and composite

structures are designed to withstand significant stresses.[63] This high threshold ensures that the sensors can continue to function and provide critical strain data even under extreme loading conditions, which is vital for real-time monitoring and early detection of damage or fatigue in critical aircraft components.

Lastly, EFPI sensors can measure the strain induced to the structure as a result of temperature or pressure, from -5000 to $+5000\,\mu\varepsilon$, indicating the capability of the sensor to determine both compressive and tensile strain.[64] Manifestation of induced-tensile strain in the composite structure may result in structural failures such as microcracking, matrix debonding, delamination, and catastrophic failure. The use of EFPI sensors is not limited to in-service damage detection but can also be utilized to monitor and assess process-induced strain. A case study of real-time monitoring of the thermal strain of CFRP composite using EFPI is reported by Leng and Asundi.[65] The sensor embedded in the midplane of the laminate was cured in the heat press machine. The result obtained indicates that the EFPI sensor can detect microdamage that occurred during the curing process.

Despite their appreciable advantage for SHM applications, FPI sensors are not easily multiplexed in their traditional form due to the fixed length of the cavity. Since the cavity length determines the specific wavelength at which interference occurs, it becomes challenging to multiplex multiple FP sensors on the same fiber without causing interference between them.[66] However, many techniques and configurations have been reported in the literature to overcome this limitation. These approaches include wavelength division multiplexing,[67] which is archivable by using different wavelengths of light for each FPI sensor, and time division multiplexing[68,69] through alternation of the time each FPI sensor is interrogated. Although these techniques enable multiplexing with FPI sensors, they may introduce instrumentation and data processing complexities. Also, a notable limitation of the EFPI sensor is its deployment in environments with extremely high temperatures. This constraint arises from the fact that many EFPI sensors utilize single-mode fibers that have a softening point of ≈800 °C. To address this challenge, research efforts have been intensifying in recent years to create EFPI sensors that employ sapphire fibers.[70] These specialized sensors are designed to withstand and measure temperatures and pressures

ADVANCED
SCIENCE NEWS
www.advancedsciencenews.com

ADVANCED
ENGINEERING
MATERIALS
www.aem-journal.com

that exceed 1000 °C. However, this might not be an essential factor for in situ SHM of aerospace composite since the component will not be susceptible to temperature of that magnitude. The maximum operating temperatures for most aerospace composites are typically below 200 °C[71]

3.1.2. Distributed Fiber-Optic Sensors

Distributed fiber-optic sensors (DFOS) are an advanced technology that has shown great promise for SHM of composite materials in aerospace applications. They are optical sensors characterized by their ability to provide a distributed measurement of parameters such as temperature and strain over long distances.[72] Based on the working principle, DFOS are categorized as optical time domain reflectometry (OTDR),[73] Raman optical time domain reflectometry (ROTDR),[74] and Brillouin optical time domain reflectometry (BOTDR).[75] OTDR relies on Rayleigh scattering, a phenomenon where light is scattered in all directions by the molecules or small particles in the medium through which it travels.[76] Light pulses are sent into the optical fiber, encountering Rayleigh scattering as they travel along the path. Also, some of the light is backscattered toward the source. The amount of backscattered light and the time it takes to return to the OTDR are measured. By analyzing the time delay and intensity of the backscattered light, OTDR can create a profile of the optical fiber. Changes in the backscattered signal can indicate events such as bends, breaks, or splices in the fiber.

Siwowski et al.[46] studied the SHM of advanced composite bridges using DFOS based on Rayleigh scattering (OTDR). The distributed strain and temperature of the bridge just after completion and before it was opened to traffic were measured, and the results obtained were validated by comparing with the experimental (obtained from foil strain gauges and vibrating wire strain gauges) and numerical results (proof load test and finite element analysis). The findings revealed the reliability of the DFOS method in monitoring the composite bridge.

Datta et al.[77] demonstrated the use of an OTDR distributed sensor, bonded along the bolt line of a composite aircraft wing-like test box, to detect disbond damage created by the removal of bolts. The results show that the system can accurately detect disbond damage irrespective of the load level, with the potential for practical application in ground-based SHM systems for aircraft and unmanned aerial vehicles (UAVs). The study concludes that the methodology holds promise for fast, efficient, and cost-effective detection of damage in aircraft structures.

Furthermore, Diaz-Maroto et al.[78] presented a study on the use of fiber-optic sensors based on distributed OTDR for strain monitoring in a composite aircraft cabin during pressurization tests. The study concluded that the sensor is a viable alternative to conventional strain gauges, offering benefits such as reduced integration and installation time, elimination of electric wires, and weight savings. The sensors effectively monitored the strain field during pressurization tests and verified the absence of structural damage, demonstrating their potential for use in aerospace structural health monitoring applications.

In contrast, ROTDR- and BOTDR-based distributed sensors leverage the principles of Raman and Brillouin scattering, respectively, to achieve distributed sensing capabilities. When photons interact with the vibrational modes of molecules in the optical fiber, they undergo a frequency shift in Raman scattering. This shift results in two components, as shown in **Figure 4**: the Stokes component, where the scattered light has a lower frequency (lower energy), and the anti-Stokes component, where the scattered light has a higher frequency (higher energy).[74,79] Therefore, pulses of light are sent into the optical fiber in ROTDR, and the Raman-scattered light, including both Stokes and anti-Stokes components, is analyzed as it returns. Thus, the frequency shift of the Stokes and anti-Stokes components determines the temperature distribution along the optical fiber.

The sensing length capability of ROTDR is ≈8 km and possesses a spatial resolution of 1 m. Unlike ROTDR, BOTDR can measure the temperature and strain of a structure up to a distance of 30 km with a spatial resolution from 1 to 4 m.[80] These features make them particularly suitable for SHM applications where continuous monitoring over extended lengths of optical fiber is required. Spatial resolution is a crucial parameter in the sensing capability of BOTDR because the resolution determines the shortest length or region where a change in temperature or strain can be accurately localized. Although there is growing research to improve the spatial resolution of BOTDR; for instance, Wang et al.[81] proposed an iterative subdivision method to improve the spatial resolution of the sensor. The approach involves a systematic division of the fiber into shorter segments, extracting sub-Brillouin signals, and iterating this process to enhance the spatial resolution of BOTDR by considering the energy density distribution and response time of the detection system.

Similarly, Almoosa et al.[82] suggested the use of an artificial neural network model to enhance the Brillouin frequency shift (BFS) resolution in differential cross-spectrum BOTDR, highlighting its flexibility, training with high-resolution data and demonstrating its effectiveness in improving BFS resolution for various pulse duration cases. Nevertheless, achieving a satisfactory spatial resolution in BOTDR involves a trade-off with the measurement range. Balancing the need for precise detection of localized events and monitoring larger sections of the aircraft structure can be challenging.

Therefore, based on the operating principle, as shown in **Table 3**, Rayleigh scattering-based distributed fiber-optic sensors
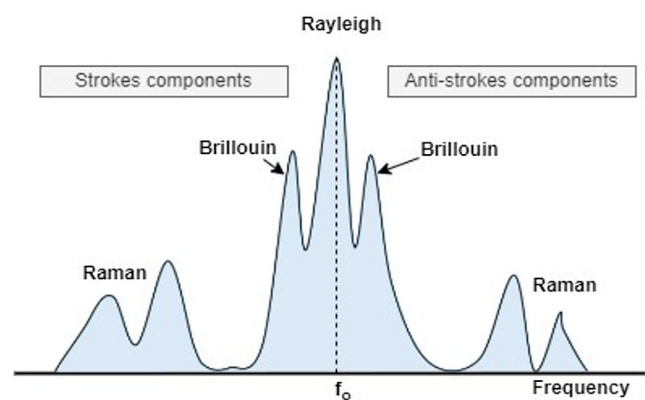

Figure 4. Schematic representation of the spectrum of backscattered light properties in the optical fiber.

Table 3. Comparison between distributed fiber-optic sensors based on operating principles.

Parameter	Raman scattering (ROTDR)[200]	Brillouin scattering (BOTDR)[201]	Rayleigh scattering (OTDR)[83]
Primary measurement	Temperature	Temperature and strain	Strain and temperature
Spatial resolution	0.1–1 m	<10 m	0.001 m
Accuracy	$\pm 1\,°C$ for temperature	$\pm 1\,°C$ for temperature, $\pm 20\,\mu\varepsilon$ for strain	High accuracy, down to $\pm 1\,\mu\varepsilon$ for strain and $\pm 0.1\,°C$ for temperature
Response time	Seconds to minutes	Seconds to minutes	Milliseconds to seconds
Sensitivity	Moderate	High	Very high
applications	Temperature profiling, fire detection, industrial process monitoring	Structural health monitoring, pipeline monitoring, power cable monitoring	Structural health monitoring, geotechnical applications, perimeter security
Damage detection capability	Limited to temperature-induced damages	Effective for both temperature and strain, suitable for detecting deformation, cracks, and other structural damages	Highly effective for detecting microstrain and minor damages such as cracks, delamination, and corrosion
Damage Localization	Moderate, depending on spatial resolution	High, precise localization of damage points	Very high, can localize small damages precisely
Environmental sensitivity	Sensitive to temperature variations, minimal strain sensitivity	Sensitive to both temperature and strain variations	Sensitive to minute changes in strain and temperature
Micromechanic failure detection	Limited, primarily sensitive to thermal effects	Effective for detecting microcracks and microstrain	Highly effective for detecting microcracks, fiber breakages, and delamination
Macromechanic failure detection	Moderate, helpful in detecting large-scale temperature variations	High, effective for detecting large-scale strain and deformation	Very high, effective for detecting large-scale cracks, delamination, and structural failures
Durability and robustness	High, suitable for harsh environments	Moderate to high, requires protection against environmental factors	High, suitable for harsh environments with protective measures
Composite material compatibility	Moderate, best suited for applications where temperature profiling is critical	High, well-suited for composite materials experiencing both strain and temperature changes	Very high, ideal for detailed strain mapping and damage detection in composite materials

(OTDR) indeed provide a comprehensive solution for monitoring the structural health of aerospace composites due to their high spatial resolution, precise damage detection capabilities, compatibility with composite materials, adaptability to harsh conditions, advanced data interpretation, and long-term durability.[83] These factors make them particularly suitable for ensuring the integrity and safety of aerospace structures, thereby enhancing performance and reducing maintenance costs.

3.1.3. Grating-Based Sensors

The fiber Bragg grating (FBG) sensor is the most established grating-based sensor, capable of demonstrating remarkable sensitivity to variations in strain, temperature, and other environmental factors.[84] Their capacity for straightforward multiplexing facilitates distributed sensing over considerable distances. At the same time, their inherent immunity to electromagnetic interference further enhances their reliability. Moreover, FBG sensors offer a compact and lightweight design, making them particularly advantageous for aircraft applications where space and weight considerations are critical.[85] Multiplexing FBG sensors along a single optical fiber allows for efficient and simultaneous monitoring of various structural deformation parameters, contributing to a comprehensive understanding of the composite structural failure.[84,86] The wavelength-encoded measurement principle of FBG sensors ensures precise and reliable data, enabling the detection of subtle changes in structural conditions. This level of sensitivity is essential for early identification of potential issues, contributing to proactive maintenance strategies and ultimately enhancing the safety and longevity of the aircraft.[87] Also, FBG sensor compatibility with existing optical fiber infrastructure facilitates seamless integration into aircraft systems. The feature streamlines the implementation process and leverages the advantages of optical fiber technology, such as high bandwidth and data transmission capabilities. Hence, these distinctive properties collectively position FBG sensors as suitable for SHM applications in aircraft structures.

The sensor (as shown in **Figure 5**) works by reflecting a specific wavelength of incident light known as the Bragg wavelength, diverting a portion of the light while allowing the remaining portion to pass through without altering its properties.[16,48] Generally, the Bragg wavelength expressed in Equation (1) is a specific wavelength of light that satisfies the Bragg condition for constructive interference within the periodic structure of the grating:

$$\lambda_B = 2\eta_e\Lambda \tag{1}$$

where λ_B is the Bragg wavelength, η_e the effective refractive index of the fiber core, and ·is the grating period.
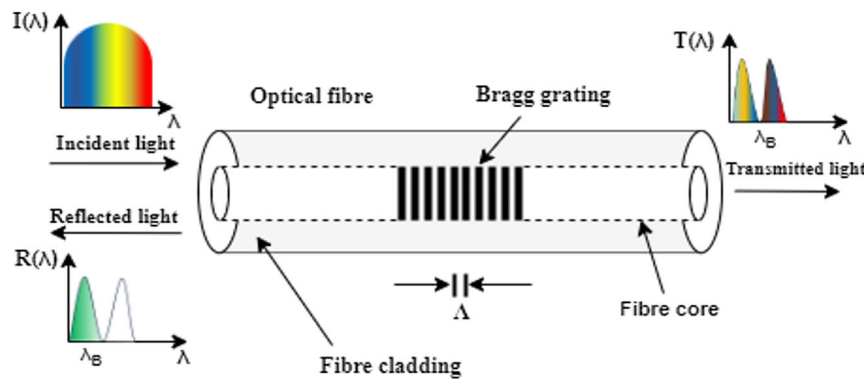
Figure 5. Working principle of FBG sensor.

In FBG sensors, the grating is a series of periodic refractive index variations along the length of the optical fiber. Therefore, when incident light with a range of wavelengths interacts with the FBG, only light that fulfils the Bragg condition (matching the periodicity of the grating) is reflected along the fiber. Thus, the Bragg wavelength serves as a reference point, and any shift in this wavelength corresponds to changes in the physical parameters (such as strain, temperature, or pressure) that FBG is designed to measure. In addition, hundreds of FBG sensors can be distributed along the optical fiber (multiplexed) and monitored without interference.[88]

As a result of the widespread adoption of FBG sensors for SHM, there is growing research interest in solving some of the problems that could influence their performance.[89] One critical area is the improvement in manufacturing technology, which permits the incorporation of sensors without any significant adverse effect on their structure and overall sensitivity. The autoclave process is the most used manufacturing technique for producing aerospace composites.[90] Due to this process's high pressure and temperature requirements, the brittle sensor might suffer deformation. Moreover, it is challenging to remove damaged sensors after curing the composite.[91] Hence, developing a suitable technique to protect the sensor and considering probable manufacturing procedures are vital. Materials, such as Teflon and polytetrafluoroethylene (PTFE) tubes with high thermal stability have reportedly been applied to the ingress/egress ends of the sensor for additional protection during the autoclave curing process.[47,48,92]

Furthermore, in a thick composite structure, lateral shrinkage may induce compressive stresses that can lead to a change in the position of the sensor and possible distortion of its response spectra.[91] One crucial means of reducing the shrinkage effect is prestressing the sensor. This process allows the peak of the FBG sensor to be at the desired position. Similarly, when a composite structure embedded with an FBG sensor is subjected to multidirectional loading, the sensor may undergo a twist due to torsional deformation, and thus, cross-sectional change occurs. The twist induced by torsional deformation can alter the effective length of the FBG sensor, impacting the strain and causing a shift in the Bragg wavelength.[93] Therefore, it is essential to consider the loading direction and how the resulting deformations affect the FBG sensor.

Generally, a light source, typically from a narrow tunable laser or wideband light source, is required to obtain the scanned Bragg wavelength (FBG interrogation). Presently, many of the technologies implemented in FBG interrogation systems (Peak Wavelength Searching and Tracking, Curve Fitting, and Zero-Crossing Algorithms) possess speed limits, thus making dynamic long-term SHM and single interrogation of large amounts of sensors complex.[91,94] While these algorithms can interpret the Bragg wavelength shift, the speed of the interrogation process is crucial in applications where rapid changes in the sensed parameters need to be captured. Advanced signal processing techniques and real-time data analysis methods (such as fast Fourier transform (FFT), digital signal processing algorithms, adaptive filtering, machine learning, and pattern recognition) may address the speed limitations.[95–98] However, the choice of a particular technique depends on the specific requirements of the application, the characteristics of the FBG sensor, and the environmental conditions. Combining multiple techniques and optimizing their parameters can lead to an effective and efficient FBG sensor interrogation system, particularly in aircraft SHM, where real-time monitoring is critical.

Another significant obstacle constraining the practical use of FBG sensors for SHM is the need for advancements in methods and equipment to achieve high-precision measurements of subtle shifts in the Bragg peaks. Commercially available optical spectrum analyzers (OSAs) exhibit a remarkable resolution of up to 1 picometer (pm), subtle temperature changes as minimal as 0.1 °C, and strains close to 1.5 µε. With relatively high prices, OSAs are limited in their application.[99] Moreover, in a situation where an accurate result is required, OSAs are unreliable and prone to wavelength calibration errors.[100]

Regarding the effect of FBG sensors on the host material, many researchers have reported that embedding sensors in the composite material can impact the mechanical properties and increase the likelihood of structural failure.[101] Factors such as the stacking angle between an optical fiber and the plies, the diameter of the optical fiber, and composite thickness influence the strength and stiffness of the material. Microcracks and delamination are initiated when the optical fiber is embedded perpendicularly to the reinforced fiber, surrounded by a polymer matrix with tiny voids. The magnitude and intensity of the defects depend significantly on the density and angle between

**ADVANCED
SCIENCE NEWS**

www.advancedsciencenews.com

**ADVANCED
ENGINEERING
MATERIALS**

www.aem-journal.com

the optical fiber and the adjacent laminate. However, manifestations of these inadequacies can be mitigated by stacking the optical fibers in a parallel direction to the reinforcing material. Regarding the issue of the diameter of the optical fibers, which are generally higher than the reinforcement (up to 10 times higher than commercially available glass and carbon fibers), thereby creating matrix-rich regions in the composite, few studies have reported the development of small-diameter optical fiber (SDOF; with outer diameters ranging from 40 to 80 μm) for SHM of FRP composite.[51,102] However, the commercial availabilities of such SDOF are scarce and expensive.

Liu, Liang, and Asundi[103] highlighted the advantages of FBG sensors, such as small size, flexibility, and resistance to heat and electromagnetic interference. Their study further discusses the fabrication of small-diameter FBGs with a core/cladding/coating diameter of 7/80/160 μm and compares them to standard fibers with a diameter of 125/250 μm. The study finds that smaller optical fibers have less impact on the mechanical performance of the host structure, and they can be used effectively for dynamic signal monitoring and are more sensitive than traditional sensors like thermocouples.

3.2. Piezoelectric Sensor

When piezoelectric materials are subjected to stress or placed in an electric field, they produce an electric charge, which can be used to study material deformation due to changes in force or displacement.[104] The distinct asymmetric crystalline structures of many dielectric materials such as polymers, quartz, and ceramics make them an ideal piezoelectric material. Hence, materials such as polytetrafluoroethylene (PTFE), polyimide, polyvinylidene fluoride (PVDF), polyvinylidene chloride (PVDC), and lead zirconate titanate (PZT) are subjected to poling for conversion to the piezoelectric material. This process involves the application of an electric field at an elevated temperature and cooling to align and polarize the internal dipoles within the materials, thus influencing their piezoelectric properties.[105] The properties are preserved in the material if they do not excite a high mechanical stress, temperature (higher than the curie temperature), or electric field capable of changing the asymmetric structure of the material to symmetric.

When used as a sensor, piezoelectric materials are versatile because they can function at a broad range of frequencies. Based on composition, piezoelectric material can be categorized as inorganic, organic, or composite-based.[106] The inorganic piezoelectric material (IPM) includes ceramics (PZT, barium titanate, lead metaniobate, aluminum nitride, lead metaniobate) and other single-crystal compounds (such as quartz, lithium niobate, langasite). Among IPM, PZT-based sensors are commonly used due to their high piezoelectric coefficient, thus offering outstanding performance.[107,108] Organic piezoelectric materials (OPM) are mostly polymers characterized with high mechanical properties. they include Polyimides (PI), Poly(vinylidene fluoride) (PVDF), Poly(lactic acid) (PLA), Polyvinylidene Fluoride-Trifluoroethylene (PVDF-TrFE), Poly(3,4-ethylenedioxythiophene) Polystyrene Sulfonate (PEDOT:PSS).[104,106] Unlike IPM, OPM possesses low density, high flexibility, biocompatibility, and easy processability. However, OPM has a relatively lower

piezoelectric coefficient than IPM, limiting their usage as sensors for SHM. Composite piezoelectric materials (CPM) are developed to improve the performance of OPM. CPM consist of polymeric piezoelectric material reinforced with IPM. Typical $BaTiO_3$/PAN membranes have reportedly been utilized for SHM of composite structures.[109] The result shows that incorporating $BaTiO_3$ nanoparticles with polyacrylonitrile (PAN) membrane improves the electromechanical property of the sensor as well as the interlaminated shear strength of the host structure. In another study, Tolvanen et al.[110] fabricated a liquid crystal polymer/PZT composite by an extrusion process for sensor applications.

Similar to fiber-optic sensors, piezoelectric sensors can easily be mounted on the surface or embedded in the structure. Surface-mounted sensors are simple to install and allow for easy removal or replacement. They are preferable for studying the deformations close to the surface of the material. However, the embedded piezoelectric sensor offers additional protection, enhanced longevity, and sensitivity to deformation.[111] Also, when the network of sensors is embedded or placed on the surface of the material, the structural performance can be compromised. Hence, sensors are connected in series or parallel, forming a continuous connection arrangement that reduces cabling length. Other piezoelectric sensors, such as Piezoelectric wafer active sensors (PWAS), have been developed and are commercially available.[112,113] PWAS consist of an array of PZT in the form of a disk or square. They are cheap and small in size compared to conventional PZT sensors. However, PWAS are brittle and may exhibit a nonlinear behavior when used at high temperatures or under intensive strain.[112]

The SHM approach using piezoelectric sensors can be achieved through active and passive methods, each with its unique set of techniques and sensors. Among the active SHM methods, Lamb wave, electromechanical impedance (EMI), and active vibration-based methods are typical.[114] These methods actively engage with the structure, employing actuators to excite it and then meticulously analyzing the responses to determine any signs of damage. Conversely, passive SHM methods, which include acoustic emission (AE), strain-based methods, and comparative vacuum monitoring, operate by passively observing the structure without the need for active excitation.[115] Therefore, active sensors are versatile devices that not only generate an output voltage in direct proportion to the strain they experience but are also capable of inducing strain when a voltage is applied. In contrast, passive sensors operate by altering their electrical resistance, optical characteristics, or magnetic properties in response to the strain exerted upon them.

In EMI, A piezoelectric transducer, such as PWAS, is attached to the structure under investigation. This transducer can act as both an actuator and a sensor (as shown in **Figure 6**).[116] Then, the transducer is connected to a low-voltage source, which leads to excitation and causes the transducer to vibrate. Due to the electromechanical coupling, the mechanical resonances of the structure are excited by the vibrating transducer. These resonances are the result of the structure's dynamic response to the input vibration. The electrical impedance of the transducer is measured over a range of frequencies. The impedance is a measure of the opposition to the flow of alternating current, and it includes both resistance and reactance.
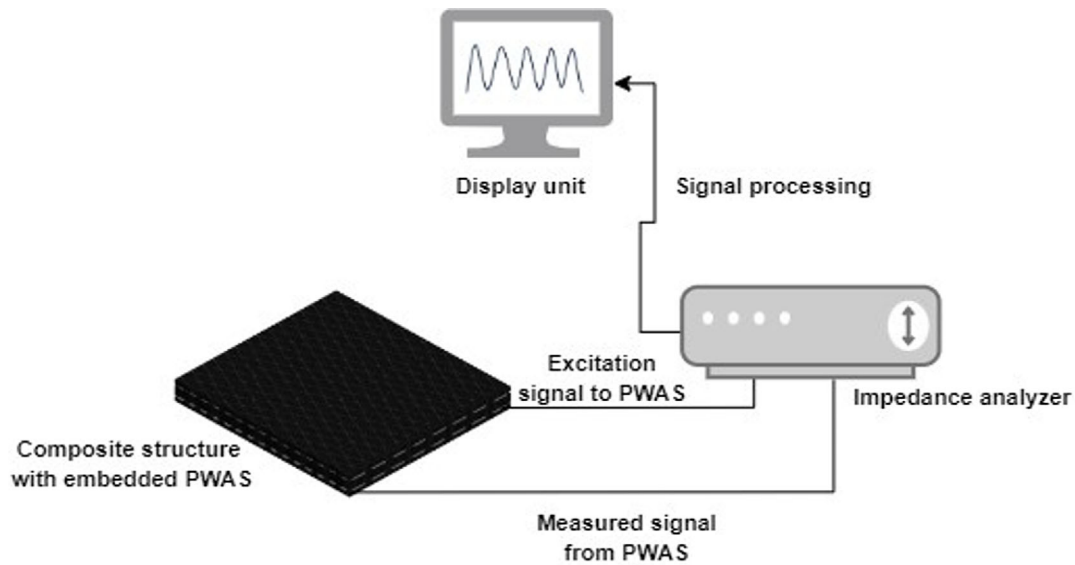
**ADVANCED
SCIENCE NEWS**

www.advancedsciencenews.com

**ADVANCED
ENGINEERING
MATERIALS**

www.aem-journal.com

Figure 6. Schematic representation of EMI sensor for SHM of composite structure.

The measured impedance is analyzed to create an impedance spectrum.[117] This spectrum reveals peaks that correspond to the mechanical resonances of the structure. Hence, the peaks are indicative of the structural integrity and can be used to assess the condition of the structure. Therefore, when damage occurs in the composite structure, it affects the stiffness and dynamic properties of the structure. This change is reflected in the impedance spectrum as shifts in the resonance peaks' frequency and magnitude. Damage indicators, as shown in **Figure 7**, are calculated from the impedance data to quantify the damage.

Generally, this approach involves measuring the EMI for the undamaged condition, referred to as the baseline signal. This baseline data is then compared with EMI signals obtained from unknown structural conditions. Any detected differences in these comparisons indicate the presence of damage.[118]

Wandowski et al.[116] reported the utilization of the EMI method to detect delamination in CFRP panels. The result indicates that CFRP delamination causes a frequency shift of a particular resonance frequency, as evident in resistance characteristics. Regarding sensitivity, typical EMI sensors possess
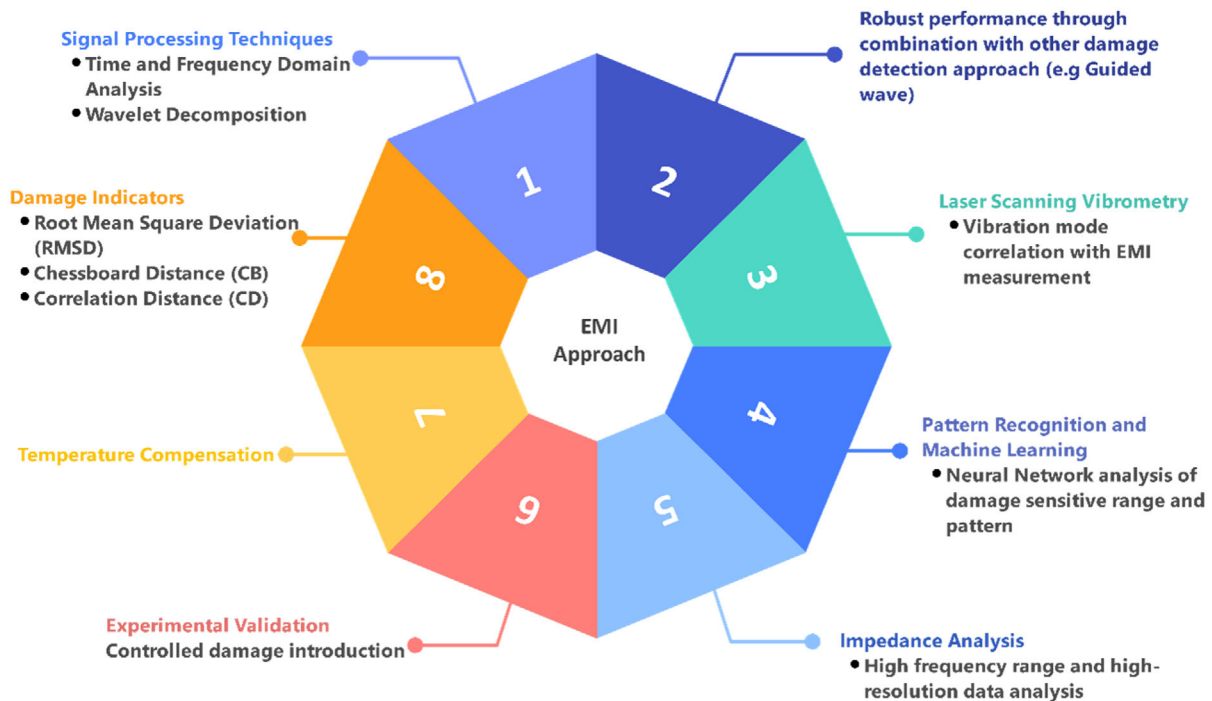

Figure 7. Multidimensional analysis techniques for damage quantification in structures using the EMI method.

high frequency (above 30 kHz). Likewise, they are immune to vibration and ambient noise and highly sensitive to minor structural damage. However, their sensitivity decreases with distance due to weak signals.[119] Therefore, EMI sensors are more suitable for localized damage monitoring of important structures prone to damage. Deng et al.[120] studied the structural debonding of CFRP concrete interface using the EMI technique and a flanged PZT patch as an actuator and sensor. The composite plate was subjected to four-point loading, while the damage degree was measured using the root mean square deviation (RMSD) and mean absolute percentage deviation (MAPD) approach. The flanged PZT (20 patches) were coated with an epoxy layer for protection and then glued to the surface of the CFRP plate. An impedance analyzer was utilized to excite the signal for the PZT. It is worth noting that EMI methods utilized in this study are susceptible to minor and incipient damage, which is preferable in determining microcracking and early signs of interfacial debonding.

Tawie et al.[121] investigate the damage detection capabilities of the EMI technique on glass fiber composite plates, focusing on various methods of attaching PZT sensors. The performance of each attachment method was evaluated using statistical metrics like RMSD, MAPD, and correlation coefficient deviation (CCD). The study found that an effective way of monitoring a thin composite structure would be to use both the RMSD and MAPD values, as the results showed that RMSD has the best R^2 values, indicating a robust linear relationship with damage progression, while MAPD values better indicated the existence of damage.

A comprehensive application of machine learning (ML) for composite damage prediction using EMI is presented by Cao et al.[122] The authors highlight the use of advanced ML models, including classical models, neural networks, and deep learning architectures like convolutional neural networks (CNNs) for direct damage prediction, which is part of the forward numerical framework. This approach is contrasted with the inverse model updating method, where the forward framework uses ML to mimic the dynamic behavior of the transducer-structure system for direct damage prediction. The authors also acknowledge challenges such as the underdetermined nature of the problem, where many damage parameter solutions may correspond to similar impedance responses, thus recognizing the need for further research to overcome such challenges.

Despite numerous studies showcasing the feasibility of the EMI technique, its practical application in aerospace composite structures has faced significant challenges. One of the most critical and complex issues is the impact of temperature on EMI signals. EMI signals are susceptible to variations in the properties of both the structure and the piezoelectric transducers. Consequently, temperature becomes a crucial factor in the performance of an EMI-based SHM system, as it can alter the material properties of both the structure and the PZTs.

As a result, researchers have explored various methods to mitigate the impact of temperature on EMI. Baptista et al.[123] propose a method to compensate for the variations in the CCD metric (CCDM) index, which is based on the correlation coefficient. The CCDM index is chosen because it appears to be less susceptible to variations in the amplitude of the EMI caused by fluctuations in the measurements. The compensation method works by shifting the frequency of the updated EMI

signature in relation to the baseline signature to maximize the correlation coefficient between them. This process is done iteratively until the maximum correlation coefficient is achieved, which indicates that the temperature effects have been compensated. Similarly, Silva, Yano, and Gonsalez-Bueno[124] proposed the transfer component analysis (TCA)-based approach to effectively compensate for temperature variations in impedance-based SHM without the need for complex computational implementations or multiple baselines. TCA, which is a subtype of transfer learning, involves transferring knowledge from a source domain, where the features data are labeled and the temperature and structural conditions are known, to a target domain, where the conditions are unknown. The technique simplifies the process by reducing the number of features. It enables the use of the same training data from a reference temperature to detect damage in different temperature conditions.

Hence, EMI method is highly effective for local damage monitoring in aerospace composites due to its sensitivity to minor structural changes. It allows for continuous real-time monitoring and early detection of damage, enhancing the reliability and accuracy of SHM systems.

In another active mode of propagation, lamb waves can be excited by the piezoelectric sensor. They are a form of elastic perturbation that can propagate in a solid plate with free boundaries.[125] These waves have wavelengths in the order of plate thickness and exhibit elliptical particle motion, both perpendicular to the surface and in the direction of propagation. Their propagation modes are divided into symmetric and antisymmetric modes.[126] In symmetric modes, particle displacement across the plate thickness is symmetrical about the median plane, meaning the motion on one side of the median plane mirrors the motion on the other side. Conversely, in antisymmetric modes, particle displacement is antisymmetric about the median plane, meaning the motion on one side of the median plane is opposite in direction to the motion on the other side. The damage detection capability of these two modes of propagation is presented in **Table 4**.

The technique, as shown in **Figure 8**, fundamentally involves examining the behavior of waves that propagate through the material and interact with its boundaries or any discontinuities, such as damage.[127] This technique relies on the comparison of the current response signal, captured after the waves have interacted with the structure, against a reference response that was recorded when the structure was known to be undamaged. Any discrepancies between the two signals can indicate the presence of damage within the structure. The PZT sensors are instrumental in both generating the Lamb waves and detecting their altered characteristics, which are then analyzed to assess the structural integrity over time.

Chen et al.[128] studied multidamage localization in the composite plate using a lamb wave-based piezoelectric transducer array. The findings show that the technique is a promising approach for damage localization in large composite structures.

Zeng et al.[129] presented a novel method for damage assessment in carbon fiber-reinforced plastic structures using a lamb wave-based approach. The method employs a statistical model (continuous hidden Markov model) for damage localization and quantification in the composite embedded with a PZT transducer and sensor to excite and receive the lamb wave signal.

Table 4. The difference between symmetric and antisymmetric lamb wave modes for damage detection.[126]

| Feature	Symmetric modes (S-modes)	Antisymmetric modes (A-modes)
Sensitivity to damage	More sensitive to through-thickness defects (e.g., delamination, deep cracks)	More sensitive to surface or near-surface defects (e.g., surface cracks, corrosion)
Signal attenuation	Lower attenuation, suitable for long-distance damage detection	Higher attenuation, limiting effective range but enhancing sensitivity to surface defects
Preferred applications	Detecting deep or extensive damage across the thickness	Monitoring surface integrity, detecting shallow cracks, corrosion, and bonding issues
Combining modes	They are often used in conjunction with antisymmetric modes for comprehensive assessment.	They are often used in conjunction with symmetric modes for comprehensive assessment.
Damage localization and characterization	Provides better detection of through-thickness defects	Enhances detection and characterization of surface and near-surface damage
Selection criteria	Selected when through-thickness integrity is critical	Selected when surface or near-surface condition is critical
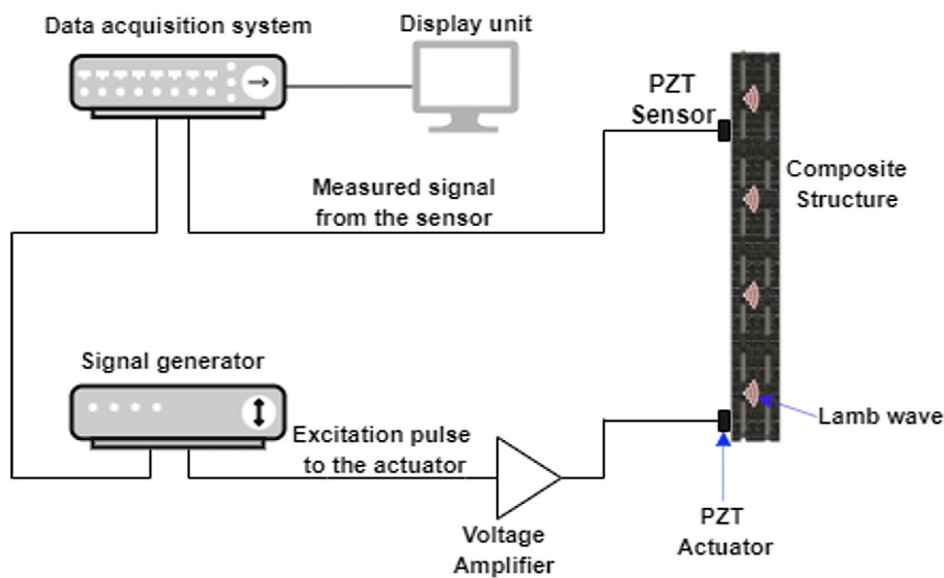
Figure 8. Schematic representation of piezoelectric sensing based on lamb wave propagation.

The study suggests that the proposed method is straightforward and efficient for damage detection in composite structures, making it suitable for in-service monitoring.

Zhang et al.[130] presented a novel approach for damage assessment in composite laminates using the Lamb wave factorization method. This method is capable of visualizing two-dimensional (2D) defects within the material by solving the inverse scattering problem, leveraging both forward and backscattering waves. The author concludes that the Lamb wave factorization method is effective for damage assessment in composite laminates and can accurately visualize defects of different shapes. The authors suggest that while a more significant number of transducers improves imaging quality, there is a trade-off between quality and measurement system complexity. They acknowledge the need for further research, especially for anisotropic or inhomogeneous materials where the dispersion curves may vary with propagation angle.

One significant advantage of lamb wave propagation, in contrast to EMI, is its capability to facilitate both local and global monitoring of structural damage.[131] Unlike EMI, which often focuses on localized areas, lamb waves exhibit the ability to travel across or through a long distance within the structure.[132] This unique characteristic allows for a comprehensive assessment of the entire system, making it particularly valuable for detecting damage in large and intricate structures such as aircraft. Using lamb waves enables a more holistic evaluation, ensuring that potential issues are not limited to specific locations. Also, the high sensitivity of this technique enables early detection of defects or cracks, facilitating timely maintenance and preventing damage progression to critical levels. Memmolo et al.[133] studied the structural assessment of impact-induced damage of composite structure using PZT transducers bonded on the plate surface to excite and sense the lamb waves. The obtained result revealed the capability of the system to detect and locate the debonded region as well as outline the depth and quantification of damage severity.

The passive mode in piezoelectric sensors is rooted in the phenomenon where the piezoelectric material responds to stress

waves or AEs.[111,134] When the material is subjected to mechanical disturbances, such as stress waves induced by external forces or AEs resulting from structural changes, the crystal lattice within the piezoelectric material deforms. This deformation leads to the generation of an electric charge due to the piezoelectric effect.

The AE passive mode has been effectively utilized to identify various damage processes in composite materials, monitor their progression, and determine their location in real-time.[10,135] This method involves the detection of transient ultrasonic waves produced by the formation of damage within the material as it is subjected to stress. Any generated AE signal carries valuable insights into the damage mechanism. This is accomplished by directly attaching piezoelectric transducers to the surface of the composite structure. PZT sensors are connected to the composite structure, as shown in **Figure 9**, and the output from each AE sensor is amplified through a low-noise preamplifier. The amplified signal is then subjected to filtering to remove any extraneous noise and is subsequently processed using appropriate electronic equipment. To ensure the efficient transmission of the acoustic signal, the AE sensors are attached to the structure using a suitable couplant, such as adhesives or grease.[136] Once firmly attached, the AE sensors capture and transform any existing stress waves within the material into electrical signals for analysis.

The AE method has been utilized to detect damage in composite structures.[135,137–140] Samborski and Korzec[141] studied the fracture resistance of FRP composites while monitoring damage onset and evolution using AE to monitor various damage phenomena such as matrix cracking, delamination, and fiber cracking. The study highlights the benefits of using the FFT to analyze raw AE signals, providing more detailed damage identification throughout the loading process. The findings show that the AE method effectively monitors damage in FRPs, and they presented illustrative examples of AE parameters' evolution against the load applied to composite specimens. Also, the study confirms the usefulness of the AE technique for damage identification in FRP composites.

Recently, Ghabarah and Ayre[142] investigated whether embedding AE sensors enhances sensitivity compared to surface-mounted sensors, considering factors like crack location and frequency. The study used two test methods: pencil lead breaking (PLB) and actuator methods, employing specific frequencies (30, 60, 150, and 300 kHz) with the actuator method. Results showed that the sensitivity of embedded sensors varied with testing methods and frequencies. Therefore, embedding AE sensors may not be advantageous for detecting low-frequency events, which are often early failure mechanisms in composites.

Despite its potential for SHM of aerospace composite, there is difficulty in accurately locating AE sources in anisotropic materials, such as fiber-reinforced composite structures.[143] Traditional localization methods, like the time difference of arrival (TDOA), struggle with the inherent variability in AE wave velocity and signal attenuation in these materials, leading to inaccurate source localization. Bhandari, Maung, and Prusty[143] proposed a novel algorithm called composite localization using response surface (COLORS) to overcome the limitations of existing methods. The COLORS algorithm is a two-step approach that utilizes a response surface model to account for the complex interactions between AE velocity profiles, attenuation rates, distances, and orientations. By doing so, the algorithm can predict AE source locations with greater precision than the conventional TDOA method. The authors demonstrate that the COLORS algorithm achieves superior localization accuracy, as evidenced by lower mean absolute error (MAE) and root mean square error (RMSE) values compared to TDOA when tested on CFRP laminated panels.

One significant difference between the AE passive mode and EMI and Lamb wave active mode is that, unlike the active sensing mechanism in which an externally acting signal is applied to the sensor, the passive sensing principle involves a piezoelectric sensor responding to naturally acting mechanical stimuli
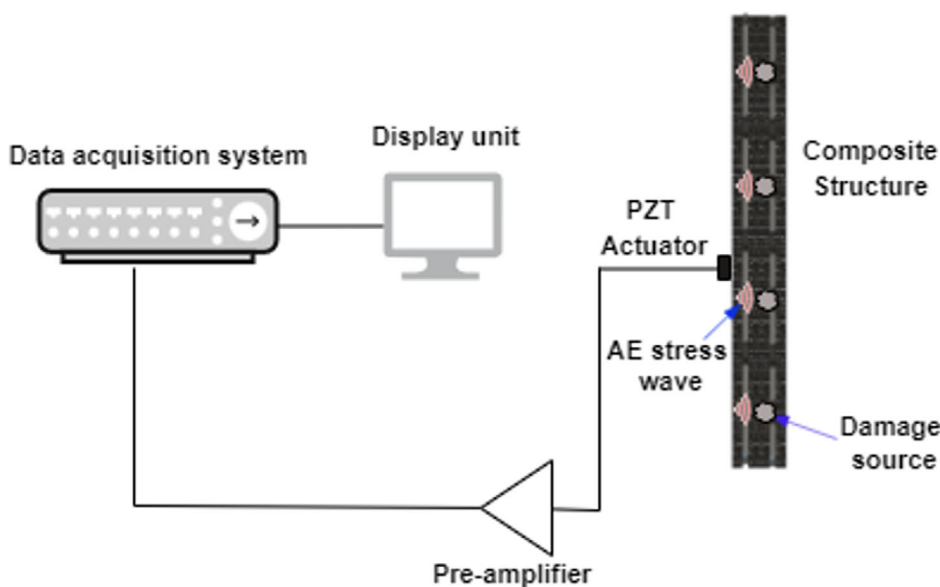

Figure 9. Schematic representation of piezoelectric sensing based on acoustic emission.

(such as AE).[144] Thus, passive sensing is well suited for continuous, long-term monitoring of gradual changes or damage that may occur during regular operational conditions.[145] In contrast, active sensing is often employed for specific investigations or inspections to monitor the response to detect any changes or anomalies.[146] Other distinctions between these sensing mechanisms are highlighted in **Table 5**.

3.3. Piezoresistive Sensing System

The word "piezoresistive" combines "piezo," meaning pressure or stress, and "resistive," referring to the change in electrical resistance. Therefore, piezoresistive sensors are derived from materials capable of undergoing a change in electrical resistance when subjected to mechanical deformation.[147] Conventional piezoresistive sensors are manufactured from metallic films and semiconductors (such as silicon or germanium) doped with impurities to introduce free charge carriers (electrons or holes) into their crystal lattice structure.[147,148] Doping alters the electrical properties of the material and makes it more sensitive to mechanical deformation. Although these conventional materials possess high piezoresistive sensitivity, their application as sensors for SHM in composite structures is impeded by some factors, notably low flexibility and stretchability.[149,150]

These limitations hinder their adaptability to composite structures' intricate shapes and dynamic deformations. Also, the reduced flexibility may result in insufficient contact with the structural surface, diminishing the accuracy and reliability of the sensor readings. The lack of stretchability limits their ability to endure varying degrees of strain and deformation, constraining their effectiveness in aerospace applications where structural components are subjected to varying impact and environmental conditions. Additionally, these materials may be more susceptible to mechanical damage due to their rigidity, compromising their longevity in SHM systems.

In contrast, composites containing conductive fibers, such as carbon, can be utilized as sensors to detect damage.[151] Therefore, when such a structure experiences damage, such as cracks, delamination, or structural deformation, the electrical resistance of the materials is altered, which serves as an indicator of damage. Unlike traditional external sensors, the sensing capability is inherent in the composite material itself, and they are generally referred to as self-sensing materials.

Self-sensing materials are a specialized category of smart materials that can be engineered by modifying their nano- and microstructures.[152] These alterations enable the materials to transduce various states of interest into measurable or observable changes. For instance, a material can be enhanced with

Table 5. Comparison between common sensing approach and their suitability for damage detection in aerospace composite structure.

Parameter	EMI[116]	Lamb Wave[125]	AE[142]
Sensing mechanism	Active	Active	Passive
Operating principle	Impedance changes due to structural damage	Wave propagation and interaction with damage	Detection of stress waves emitted by damage
Piezoelectric sensor type	PZT patches	PZT patches	PZT sensors or other piezoelectric materials
Frequency range	High-frequency (typically 30 kHz–1 MHz)	Low to high-frequency (typically 10 kHz–1 MHz)	High-frequency (typically 20 kHz–1 MHz)
Signal type	Impedance measurement	Ultrasonic waves	AE signals
Damage types detected	Cracks, delaminations, debonding	Cracks, delaminations, debonding	Cracks, fiber breakage, delaminations
Sensitivity	High	High	High
Localization capability	Limited (requires multiple sensors)	Good (with proper sensor network)	Excellent (with proper sensor network)
Integration with structures	Easy	Moderate	Easy
Real-time monitoring	Yes	Yes	Yes
Environmental influence	Affected by temperature and humidity	Affected by temperature and humidity	Affected by noise, temperature, and humidity
Typical applications	Local damage detection, health monitoring	Global structural health monitoring, damage localization	Event detection, structural health monitoring
Coverage area	Localized (near the sensor)	Wide area (depending on wave propagation)	Localized (near the event)
Interference susceptibility	Low	High (due to wave reflections and scattering)	High (due to external noise)
Material compatibility	Compatible with various composites	Compatible with various composites	Compatible with various composites
Long-time stability	High	High (if environmental effects are controlled)	Moderate to High (affected by sensor placement and environmental conditions)
Reliability	High	High (with proper system maintenance)	Moderate to High (dependent on noise and event detection accuracy)

**ADVANCED
SCIENCE NEWS**

www.advancedsciencenews.com

**ADVANCED
ENGINEERING
MATERIALS**

www.aem-journal.com

piezoelectric properties to convert mechanical stress into electrical charges. Alternatively, it can be functionalized with specific electrical properties to transduce mechanical strain into a detectable change in an electrical signal. The primary measurement principle of self-sensing materials involves detecting an electrical signal that corresponds to a change in the material's geometry.[153] For example, by measuring the resonant frequency of a material, any changes can be correlated to variations in mass or stiffness. Hence, the principle behind creating resistance-based self-sensing materials involves transforming the structural component of interest into a strain gauge.

The principle of resistance-based self-sensing composite components can be achieved by transforming the material into a strain gauge. Consider a single CFRP composite with the fiber subjected to uniaxial stress, as shown in **Figure 10**.

The electrical resistance of the carbon fiber before deformation can be expressed as:

$$R = \rho L / A \tag{2}$$

Where ρ is the resistivity of the carbon fiber, L is the length, and A is the cross-sectional area ($A = \pi r^2$).

At a small deformation of σ and taking the derivative of the natural logarithm of the electrical resistance, then Equation (1) can be expressed as:

$$\frac{1}{R}\frac{dR}{d\sigma} = \frac{1}{\rho}\frac{d\rho}{d\sigma} + \frac{1}{L}\frac{dL}{d\sigma} - \frac{1}{A}\frac{dA}{d\sigma} \tag{3}$$

$$\frac{dR}{R} = \frac{d\rho}{\rho} + \frac{dL}{L} - \frac{dA}{A} \tag{4}$$

For the cross-sectional area:

$$\frac{1}{A}dA = \frac{1}{A}d\pi + 2\frac{1}{r}dr \tag{5}$$

Hence,

$$\frac{1}{A}dA = 2\frac{dr}{r} \tag{6}$$

Substituting Equation (6) into Equation (4):

$$\frac{dR}{R} = \frac{d\rho}{\rho} + \frac{dL}{L} - 2\frac{dr}{r} \tag{7}$$

Therefore, Equation (7) can be expressed in terms of elastic strain where ε is the longitudinal strain and ε_r is the radial strain:
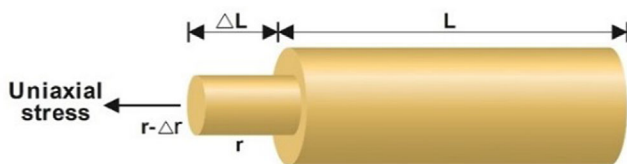

Figure 10. Schematic representation of self-sensing carbon fiber strain gauge under uniaxial stress.

$$\frac{dR}{R} = \frac{d\rho}{\rho} + \varepsilon - 2\varepsilon_r \tag{8}$$

Likewise, by expressing Equation (8) in terms of gauge factor (GF = $(dR/\rho\varepsilon)$) and taking the poison ratio, $v = -\varepsilon/\varepsilon_r$

Thus, the GF for the CFRP composite in terms of Poisson's ratio and resistivity change is:

$$\text{GF} = (1 + 2v) + \frac{d\rho}{\rho\varepsilon} \tag{9}$$

The derivation of Equation (9) expresses how the GF of a single CFRP composite can be expressed in terms of its geometric changes and piezoresistive effect.

The first term $(1 + 2v)$ represents the variation in the carbon fiber resistance due to geometrical changes when the composite material is subjected to mechanical strain, the length and cross-sectional area of the carbon fiber change. The factor 1 accounts for the linear change in length, while the term $2v$ accounts for the change in the cross-sectional area. This change in geometry affects the electrical resistance of the fiber. The second term $(d\rho/\rho\varepsilon)$ represents the piezoresistive effect, which is the change in the electrical resistivity of the carbon fiber due to applied mechanical strain. The term $d\rho/\rho$ signifies the relative change in resistivity, and when divided by the strain ε, it shows how much the resistivity changes per unit strain.

In practical applications, these relationships are crucial for developing a self-sensing composite material system. The signal processor attached to the composite material receives electrical signals indicating the resistive strain (changes in the resistance of the carbon fiber). By using the GF formula, the signal processor can correlate these electrical resistance changes to the mechanical strain experienced by the composite material.[154]

One of the shortcomings of converting structural composite into strain gauge is due to the low sensitivity of the strain that results in impractical applicability of the self-sensing principle, especially for composite reinforced with nonelectrically conductive fibers such as glass and aramids.[153] Hence, the nano- or microstructure of the components can be modified to attain electrical percolation.[155]

Electrical percolation refers to the phase transition in a material marked by a significant change in its electrical conductivity. This transition occurs when a composite is loaded with electrically conductive nano- or micro-particles to a point where conductive pathways form throughout the material. As these conductive chains are established, the composite's conductivity dramatically increases (or its resistivity decreases).

A series of recent studies have proposed the incorporation of conductive nanomaterials (CNM) (such as carbon nanotube (CNT) and graphite and graphene nanoplatelets) into the composite to improve damage sensing, strain monitoring, and mechanical strength of the structure.[156–159]

Kostopoulos et al.[160] studied damage sensing capabilities of carbon fiber-reinforced laminates functionalized with multi-walled CNT (MWCNT). Varying percentages by weight of the MWCNT were dispersed in epoxy polymers at a high shear force to ensure homogeneity of the mixture, then sixteen plies of unidirectional carbon fibers were incorporated into the Epoxy/MWCNT blend by wet infiltration method, after which the

composites were cured in an autoclave. Results indicate that incorporating CNT into the composite enhances the mechanical properties and sensitivity of the material to tensile loading. During deformation, the composite undergoes resistance change due to corresponding dimensional alterations. Also, the study reveals that fiber failure and fiber-matrix debonding affect the strain field sensed by the CNT network due to changes in the matrix conductivity.

Similarly, Tzounis et al.[161] developed an ultrasensitive CNT-modified glass fiber for SHM of composite laminates. A suspension of CNT was coated on a surface of unidirectional glass fiber using a wet chemical deposition technique. Subsequently, a composite panel was manufactured by vacuum infusion of the CNT-doped glass fiber unidirectional (UD) prepreg with a blend of epoxy resin and a hardener. The finding revealed that incorporating the CNT/glass fiber into the matrix increases the electrical conductivity of the composite. Also, the self-sensing property of the material improves, as evident by the double cantilever beam (DCB) test, which indicates a step increase in the resistance due to the progressive growth of composite delamination. Luo et al.[162] proposed the development of a conductive single filament sensor for SHM of composite material. Different types of fibers (glass, polyaramid, nylon, and polyethene-terephthalate) in single filament form were modified with SWCNT by spraying coating technique to form a thin film fiber sensor. Then, the sensors were incorporated between layers of plain-woven fiberglass prepreg and cured with a hot press. Piezoresistive sensing properties of the composites were determined by subjecting them to coupled electrical-cyclic tensile testing. The findings indicate the sensor's ability to discover micro-cracking initiation and propagation in the host composite. However, it is essential to note that the sensors' resistivities are greatly influenced by their position in the composite, the inherent properties of the fiber substrates, and the degree of CNT coating. A further novel finding for SHM of polymeric composite by evaluating the piezoresistivity of a thin film graphite nanoplatelet (GNP) sensor was proposed by Luo and Liu.[163] A one-dimensional fiber sensor was fabricated using a continuous roll-to-roll spray coating process and embedded in an epoxy/glass fiber laminate before curing in the oven. The piezoresistive response of the sensor to cyclic tensile strain revealed a linear increase in resistance with a corresponding increase in strain within the elastic region of the composite (i.e., the sensor is sensitive to applied strain). Likewise, the ability of the sensor to monitor damage was noticeable at a high strain rate due to a decrease in sensor resistance compared to the elastic zone (attributed to crack initiation and delamination growth propagation), further by step increase in sensor electrical resistance as the composite undergoes catastrophic failure (i.e., fiber breakage).

Generally, the piezoresistive sensing ability of CNM can be traced to their electrical properties, which are highly dependent on their atomic structure. When CNM undergoes deformation or chemical doping, their electrical resistance changes due to alteration in their atomic structure.[164] Moreover, the dispersion of the CNM within matrix-rich regions of the composite establishes percolating networks between the matrix and the fibers, thus enhancing both the mechanical strength and strain sensitivity of the host structure.[165] Another significant benefit of utilizing CNM as reinforcements in composite materials is their diminutive size, which allows them to be incorporated into the matrix without inducing damage or initiating micro defects at a low percolation threshold.[166]

While the addition of CNM to composite structures has been shown to enhance their self-sensing capabilities, the processing methods employed for CNM incorporation are also crucial determinants of the structures' piezoresistive sensitivity. The choice of processing technique significantly impacts the dispersion, alignment, and connectivity of CNM within the polymer matrix.[167] Conventional processing methods, such as melt mixing and solution casting, often result in nonuniform CNM dispersion and agglomeration in the composite, leading to limited piezoresistive sensitivity.[168] However, advanced processing techniques, such as electrospinning, template synthesis, and in situ polymerization, enable the formation of well-aligned and interconnected CNM networks, substantially improving the piezoresistive performance of the composite.[169] Moreover, optimizing processing parameters, such as temperature, viscosity, and shear rate, can further refine the CNM dispersion, thus improving the sensing capability of the composite.[170] Therefore, careful optimization of processing techniques is essential for achieving the desired piezoresistive properties in CNM-reinforced composite structures. **Table 6** summarizes some commonly utilized techniques

Table 6. Commonly utilized techniques for improving the piezoresistive sensitivity of composite structures.

CNM	Reinforcement	Polymer matrix	Incorporation/Processing technique	Mechanical test
MWCNT[202]	Carbon fiber	Epoxy	Electrospinning of piezoresistive fiber containing a solution blend of MWCNTs, PMMA, and DMF onto a polished surface of CFRP and subsequent curing in an oven	(a) Quasi-static flexural test. (b) Dynamic vibration test
GNP[203]	Glass fiber	Epoxy	Spray coating of GNP/ethanol on glass fabrics and vacuum-assisted resin infusion of epoxy resin	(a) Flexural test. (b) Interlaminal shear strength
SWCNT[161]	Glass fiber	Epoxy	Wet chemical deposition of SWCNT on UD glass fabrics and vacuum infusion of epoxy resin	Mode I DCB tests
MWCNT[160]	Carbon fiber	Epoxy	Direct mixing of MWCNT in epoxy matrix and wet infiltration with carbon/epoxy UD laminates	Monotonic and cyclic tensile test
SWCNT[204]	Glass fiber	Epoxy	Fabrication of SWCNT smart-sensing bucky paper by filtration and incorporation of woven glass fabrics with subsequent vacuum infusion of epoxy resin	Tensile test
MWCNT[205]	Glass fiber	Vinyl ester	Electrophoretic deposition of MWCNT on the glass fabric surface and oven curing of vinyl ester with an embedded monofilament of MWCNT/glass fiber	Tensile test

**ADVANCED
SCIENCE NEWS**

www.advancedsciencenews.com

**ADVANCED
ENGINEERING
MATERIALS**

www.aem-journal.com

for improving the electrical conductivity and enhanced piezoresistive sensitivity of composite structures.

Despite its simplicity of integration and lightweight compared to other SHM methods, improved mechanical properties, and sensitivity to intra-and-interlaminar failure, the piezoresistive sensing method is currently limited to laboratory scale. Hence, improvement for SHM of large-scale structures is required. Accurate positioning of the electric circuit for optimum development of the detection grid, as well as separation of sensing signal resulting from the CNM network and the conductive fibers (CFRP), is another challenge. Many research findings have shown promising results in the location of damages in composite structures through the incorporation of CNM.[171–175] However, increased viscosity and inhomogeneous dispersion of CNM in the composite polymer matrix are of great concern. Hence, advanced manufacturing techniques such as electrospinning, 3D printing, and in situ polymerization can create more uniform sensing patterns, improve dispersion and alignment of piezoresistive materials. By integrating these materials into the critical areas of the aircraft, any strain, stress, or damage can be detected early, allowing for timely maintenance and reducing the risk of catastrophic failures.

4. Sensing System Challenges and Potential Solutions for Effective Structural Health Monitoring of Aerospace Composite

An effective SHM system seamlessly integrates the sensing system and the interrogation unit to provide continuous, real-time monitoring of structural integrity. The sensing system, comprising the sensing material and its subcomponents (probe, conditioning unit, bondline, and sealant), ensures accurate and reliable detection of physical changes in the structure. The interrogation unit processes and evaluates these signals to provide actionable insights into the health of the structure, ultimately enhancing safety, reliability, and maintenance efficiency.[176]

Generally, SHM system requirements for aerospace composites, as shown in **Figure 11**, include lightweight, high performance, reliability, availability, and cost-effectiveness. The performance of SHM systems must significantly surpass that of conventional NDE techniques to be considered viable replacements. Key performance metrics include sensor sensitivity for detecting damage, compatibility with the composite materials to avoid adverse effects on structural integrity, as well as high accuracy and resolution for monitoring damage size and growth.[177] Additionally, the system should be capable of monitoring a wide range of composite failure modes using the same interrogation unit and sensors. The correlation between sensors and interrogation units is fundamental to the effectiveness of SHM systems for aerospace composites.

For the sensor, the top requirement is how the device will be connected to the aerospace composite components. Likewise, the size and complexity are crucial, especially in relation to calibration within the composite structure.

In aerospace applications, bonding sensors onto the surface of the structure is often more desirable than embedding or sandwiching them between the component.[178] This approach is significant in terms of simplicity in installation/general maintenance, scalability for reconfiguration, noninvasiveness,
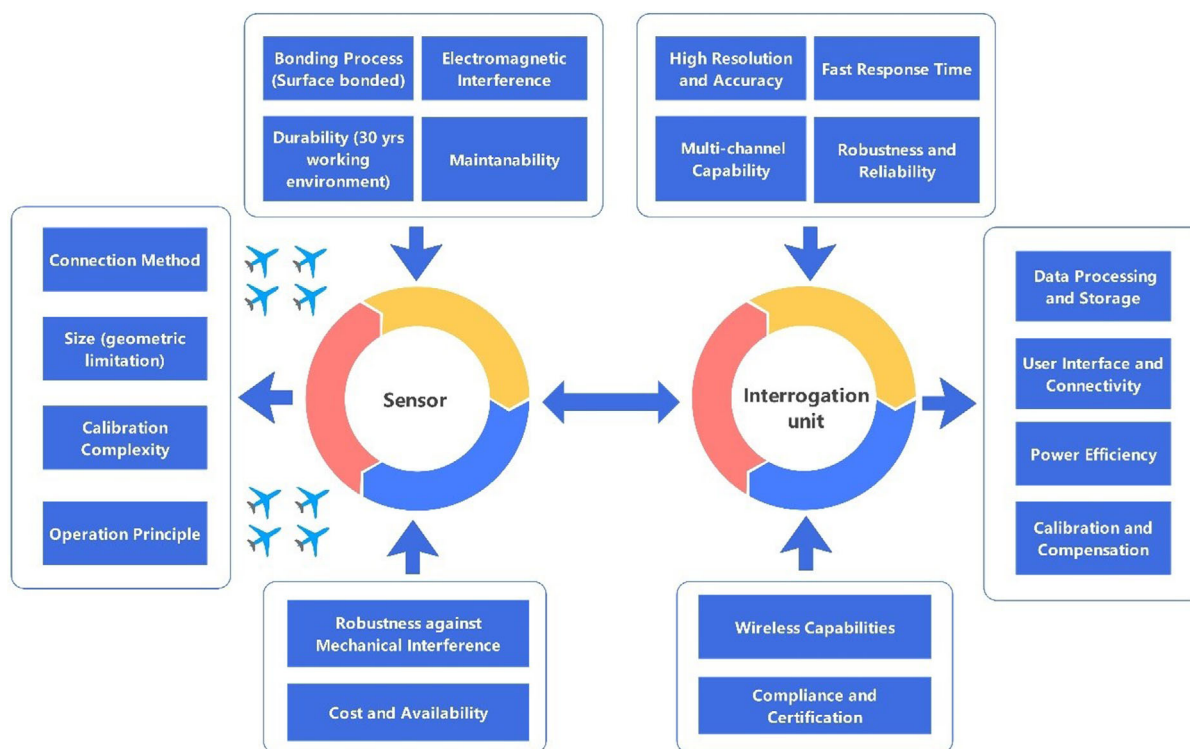

Figure 11. Structural health monitoring system requirements for aerospace composite.

improved signal quality, cost-effectiveness, and targeted monitoring capability.

Although a substantial body of work on SHM sensors research has diligently tackled deployment challenges,[179,180] it is imperative to address lingering issues that impede their seamless integration into monitoring systems. While many of the optical fibers discussed in this study can be bonded onto the surface of the structure, a few challenges still need to be solved. For instance, maintaining the durability and longevity of FBG sensors bonded onto the surface of an aerospace composite component subjected to a harsh environment is challenging due to exposure to high stresses, temperature variations, and potential chemical exposure. However, developing robust protective coatings and packaging materials to shield the sensors from environmental factors without reducing their sensitivity, as well as conducting extensive testing to validate the sensor longevity under operational conditions, is one way to solve this problem. The primary concerns are ensuring that the coating does not introduce additional strain to the fiber and that it does not significantly alter the optical properties of the sensor. Hence, the coating process must be carefully controlled, and the materials are selected based on their compatibility with the FBG sensor and the expected environmental conditions. The goal is to achieve a balance between protection and sensitivity, allowing optical fiber sensors to maintain their accuracy and reliability over the long term in various SHM applications. The coating materials such as polyimide, acrylate, and ORMOCER have reportedly been utilized to successfully bond FBG sensors with a composite structure with high reliability and without interference with the sensor sensitivity.[181–183]

Another pertinent challenge that primarily affects both the fiber-optic sensors and the piezoelectric sensors (for both active and passive monitoring approaches) is the issue of temperature change, which might affect the strain measurement. Therefore, accurate calibration of these devices is essential for reliable and efficient temperature compensation techniques. For instance, a reference sensor or separation temperature sensing alongside a strain sensor can be used to measure strain and temperature effects. Likewise, the interrogation unit can also be calibrated to provide temperature compensation for the temperature/strain signal received from the sensor.

Furthermore, the continuous availability of data collected from sensors in SHM systems offers numerous advantages over conventional NDE techniques, including real-time monitoring, early damage detection, long-term trend analysis, improved safety, and cost-effectiveness. This makes SHM an essential tool for modern infrastructure management and maintenance.

However, the SHM system for aerospace composite components generates vast amounts of data due to the complexity and anisotropic nature of the material, coupled with the need for continuous real-time monitoring. Storing this continuous influx of large datasets, especially over long periods, requires efficient storage and data management solutions. Key challenges include data compression and handling missing or corrupted data. Hence, successful implementation, management, and efficient processing of these data are vital and indispensable.

A viable approach to managing dataset from SHM system is to enhance the computing power of the interrogation unit with other powerful cloud and edge computing components, such as the embedded processors or microcontroller, digital signal processors, field-programmable gate arrays, ML accelerators, real-time operating systems, memory and storage, communication modules, and other ML framework. When these components are integrated with the interrogation unit, it performs additional tasks such as advanced data preprocessing, real-time anomaly detection, and feature extraction before transmitting data to the cloud. This approach reduces the volume of data sent to the cloud and allows for faster local decision-making (**Figure 12**).

As sensors are deployed on aerospace composite components to monitor parameters like strain, stress, and vibration, the interrogation unit equipped with edge computing capabilities aggregates these data streams. The initial stage involves real-time data preprocessing, including noise filtering, removing irrelevant data, and detecting potential anomalies. Primary data analysis occurs at this phase, ensuring only crucial features, such as frequency patterns or potential damage indicators, are forwarded for further analysis. This reduces the data load sent to the cloud, improving efficiency.

After preprocessing, the system initiates data transmission to the cloud. This step is facilitated by secure communication protocols, often using 5 G, satellite communication, or other wireless technologies. The system prioritizes the data based on criticality; urgent data, such as anomaly reports, are transmitted immediately, while less critical data is queued for periodic upload. Data compression techniques are applied to reduce bandwidth consumption during transmission, ensuring efficient use of network resources.

Once in the cloud, the data are stored in a scalable cloud storage platform that supports long-term storage and secure access. These cloud platforms, like AWS or Azure, employ robust data integrity and security protocols to protect SHM data from unauthorized access and corruption. The scalable infrastructure ensures that the vast amounts of data generated over the aircraft's lifecycle are securely stored.

In the cloud, advanced ML and artificial intelligence (AI) algorithms analyze the data to identify trends, correlations, and early signs of structural failure. This level of processing involves computationally intensive tasks, such as predictive analytics, to estimate the remaining useful life of components or data fusion, which integrates data from multiple sources for comprehensive analysis. This ensures that subtle patterns or emerging damage are detected early, allowing maintenance teams to intervene before critical failures occur. Processed data from the cloud is visualized in real-time dashboards that provide engineers and maintenance teams with an intuitive overview of the aircraft's structural health. These dashboards can feature 3D models highlighting areas of concern and allow for the generation of custom reports. These reports help maintenance crews take preventive actions, such as scheduling inspections or repairs based on data-driven insights.

In addition, a feedback loop sends updated insights back to the edge devices, allowing them to fine-tune their local algorithms for more accurate anomaly detection during future flights. This ensures continuous improvement in data processing and decision-making at the edge level.

Finally, the SHM system is integrated with the broader aircraft maintenance management system (MMS). This integration enables proactive and condition-based maintenance, reducing the
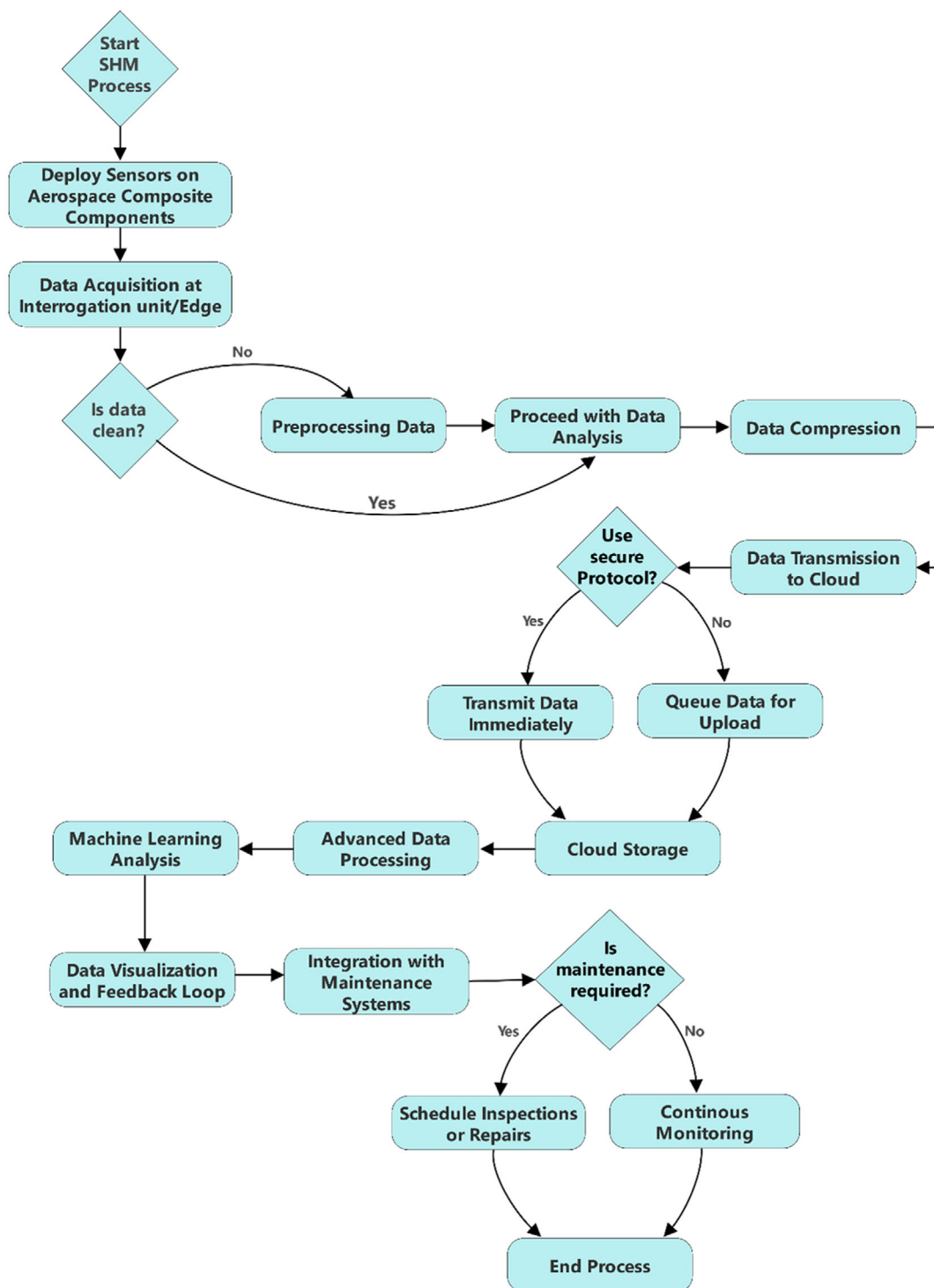
**ADVANCED
SCIENCE NEWS**

www.advancedsciencenews.com

**ADVANCED
ENGINEERING
MATERIALS**

www.aem-journal.com

Figure 12. Decision tree for managing large-scale data in SHM systems.

need for reactive repairs. By directly linking the SHM data to maintenance schedules, the system ensures that potential structural issues are addressed before they escalate into safety concerns.

The cloud platform's ability to analyze large-scale data and provide meaningful insights, combined with the edge system's local processing power, results in a more responsive, efficient, and intelligent SHM system. This integration improves aircraft safety and extends the lifecycle of critical components, providing real-time insights and long-term data archiving for continuous structural monitoring.

Xinlin et al.[184] presented the use of ML for quantitative analysis of damage in composite structures using an AE sensor. Mohapatra et al.[185] utilized a similar machine-learning approach to estimate load distribution on suspension bridges using FBG sensors and IoT. Azad et al.[15] provided an in-depth analysis of the application of AI techniques in SHM of composite structures.

The development of a self-sensing system utilizing piezoresistive technology is a promising trend for effective SHM in large aerospace components, particularly as leading aircraft manufacturers like Boeing and Airbus increasingly incorporate advanced composite materials to enhance weight reduction, fuel efficiency, and aerodynamic performance.

Achieving a uniform distribution of piezoresistive materials within the composite matrix can be difficult, potentially leading to inconsistent sensor performance. Furthermore, electrical signals from piezoresistive and AE sensing can be affected by noise and interference from other aircraft systems. However, the use of advanced fabrication techniques such as electrospinning, 3D printing, and inkjet printing to create more uniform and precise sensing patterns within or on the surface of the composite materials is a promising solution for the uniform distribution of sensing material in the composite structure.[186] Likewise, by implementing noise reduction techniques such as shielding, filtering, and differential measurement methods, signal quality can be improved **Table 7**.[187]

5. Integration and Implementation in Aerospace: Aligning with Industrial Standards for Enhanced Performance

To ensure the widespread adoption of SHM systems in the aerospace industry, these systems must be capable of integrating seamlessly with new and existing industrial standards. Achieving this requires a multifaceted approach that focuses on communication protocols, modularity, data management, ruggedization, integration with certification processes, and the use of advanced technologies such as AI (**Figure 13**). By addressing these factors, SHM systems can become indispensable tools for ensuring the long-term health and safety of aerospace composite structures.

One of the critical factors in integrating SHM systems into the aerospace industry is the standardization of communication protocols. Given the variety of sensors used for monitoring composite structures, ranging from piezoelectric to fiber-optic sensors, ensuring uniform communication is vital. Adopting established communication standards such as IEEE 802.15.4 or Bluetooth Low Energy (BLE) would facilitate intersensor communication across an aircraft's monitoring system.[188] These protocols, which are both low-power and reliable, would help ensure seamless integration with the data acquisition systems commonly used in modern aircraft. Aligning these communication systems with aviation-specific standards such as ARINC 429,[189] the framework used for transmitting data between avionics systems would allow SHM sensors to be compatible with existing aircraft monitoring and diagnostic infrastructure. By adopting standardized communication protocols, SHM systems can facilitate real-time structural health monitoring, enabling early detection of issues such as cracks, delamination, or material fatigue and reducing the risk of catastrophic failure.

Furthermore, for efficient scalability and widespread adoption, the SHM system must be modular and easily adaptable to both new and existing aircraft. A modular system allows for the integration of a variety of sensors tailored to specific needs. For instance, recently, SMARTWISE consortium, in collaboration with Airbus, developed an autonomous wireless sensor that operates based on the principle of passive and active piezoelectric

Table 7. Sensor challenges and potential solutions for SHM of the aerospace composite structure.

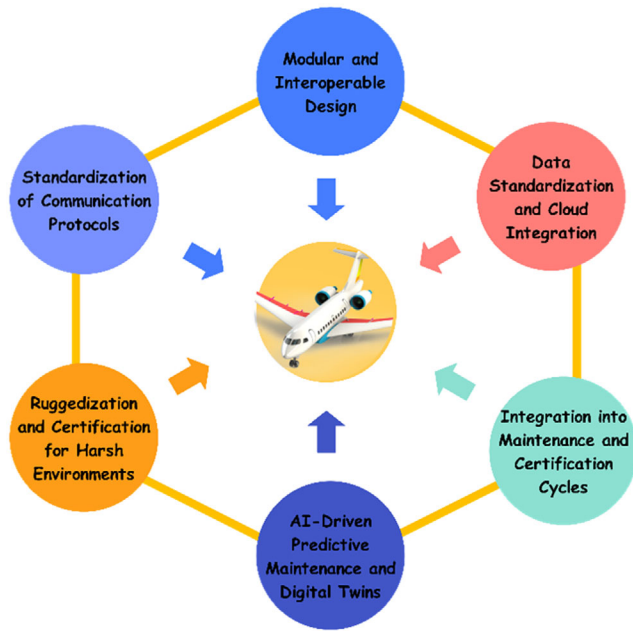| Sensor type	Challenges	Potential solution
Interferometric sensor[206]	(a) Precise alignment required. (b) High sensitivity to temperature and vibration. (c) Noise from external sources. (d) Accurate calibration required. (e) Protective coating required. (f) Large data volumes, real-time processing. (g) Compatibility with existing avionics	(a) Precision alignment tools, automated placement systems. (b) Automated calibration and temperature compensation. (c) Advanced algorithms and ML for effective data processing. (d) improved sensor housings, protective coatings
Distributed sensor[207]	(a) Complex optical pathways. (b) Sensitivity to noise and environmental changes. (c) Complex calibration, temperature compensation. (d) High data rates, complex analysis	(a) Improved OTDR technology, robust optical fibers. (b) Integrated networks for distributed sensing. (c) Advanced calibration algorithms, environmental compensation. (d) Big data analytics, real-time processing. (e) Durable optical fibers, protective coatings
FBG sensor[208]	(a) Proper alignment and bonding. (b) Sensitive to temperature variations. (c) Noise from optical sources. (d) Long-term stability of optical fibers. (e) Compatibility with avionics, maintenance systems	(a) Enhanced integration techniques with protective coatings for optical fibers. (b) Efficient data processing, ML. (c) Automated calibration and temperature compensation
Piezoelectric sensor[209]	(a) Correct placement and bonding. (b) Temperature. (c) Humidity sensitivity. (d) Electromagnetic interference. (e) Fatigue resistance of piezoelectric materials. (f) Sensitivity calibration, temperature effects. (g) High-frequency data processing, real-time monitoring	(a) Advanced bonding methods, durable materials. (b) Automated sensitivity calibration, temperature sensors. (c) Real-time signal processing, AI-based analysis. (d) Robust materials, protective encapsulation. (e) Networked piezoelectric sensors
Piezoresistive self-sensing system[210]	(a) Uniform distribution of materials. (b) Electrical noise, signal interference. (c) Long-term stability and protective coatings. (d) Calibration and sensitivity to small strain changes. (e) Managing large data volumes	(a) Electrospinning, 3D printing for uniform distribution. (b) Automated calibration, temperature compensation. (c) ML for pattern recognition. (d) Protective coatings, durable composites

**ADVANCED
SCIENCE NEWS**

www.advancedsciencenews.com

**ADVANCED
ENGINEERING
MATERIALS**

www.aem-journal.com

Figure 13. Core elements for seamless integration of SHM systems in aerospace composite structures.

sensing.[190] The designed modular wireless nodes can process large deformation datasets from multiple sensors with network architecture 60% lighter than many of the conventional wired systems. This diversity is vital due to the diversity of composite materials utilized in modern aerospace structures. Also, the modular SHM system must be interoperable, such that sensors from different manufacturers are compatible with the same aircraft system without substantial recalibration. Likewise, the sensor must be interoperable with existing NDE diagnostic tools to streamline maintenance processes.

Regarding data standardization and cloud integration, the SHM system collects large datasets over time. Thus, ensuring accessibility and standardization is vital. By using cloud-based platforms, as discussed above, SHM sensors can store and process vast amounts of data while complying with aerospace safety regulations such as DO-326 A for cybersecurity in civil aviation systems and DO-178C for software.[191] These standards ensure secure transmission and processing of data, minimizing cyber-attacks or data corruption risk. Similarly, standardizing the data formats will make integration into existing MMSs seamless. The MMS is developed to handle predictive maintenance scheduling and cloud integration for real-time analysis of structural integrity. Hence, compliance with certification standards is ensured, and aircraft safety is improved.

Aircraft are subjected to harsh environmental conditions, such as wide temperature ranges, mechanical stress, and electromagnetic interference. Therefore, a rugged SHM sensor is essential to withstand these challenges. The aerospace industry follows stringent guidelines such as RTCA DO-160 G, which defines environmental conditions for electronic equipment installed on aircraft, including temperature, pressure, vibration, and shock resistance.[192] Adherence to this standard ensures the reliability of SHM systems in high-stress environments.

High-temperature piezoelectric materials and fiber-optic sensors are designed to operate under these extreme conditions without compromising accuracy or functionality. By adhering to these stringent certification requirements, SHM systems can provide reliable data, even in the harsh environments encountered by aerospace composite structures.

Similarly, SHM systems need to align with existing maintenance and certification cycles within the aerospace industry. By providing continuous, real-time monitoring of composite structure, the SHM system has the potential to transform conventional manual inspection operations, thus reducing the need for time-consuming manual inspections. Moreover, they could integrate perfectly with existing FAA Part 23/25 certification processes for aircraft airworthiness by offering continuous structural integrity data that support compliance with safety regulations.[193]

Finally, the integration of AI into the system offers a powerful tool for predictive maintenance as a result of vast data analysis capabilities.[194] This proactive approach allows engineers to address potential problems before leading to significant damage. Likewise, digital twin technology allows the creation of a virtual replica of the aircraft (3D models), allowing for real-time simulations and monitoring of structural health. These two tools not only enhance safety but also improve the efficiency of maintenance schedules, ensuring that the SHM systems remain aligned with evolving aerospace safety standards.

6. Conclusion

The present study provides an in-depth analysis of the current state of technology and research in the field of SHM for aerospace composite materials. The review highlights the critical role of SHM in ensuring the safety, reliability, and longevity of aerospace structures, given the increasing use of advanced composite materials in the industry. These materials, while offering significant advantages over conventional metals in terms of strength-to-weight ratio and design flexibility, present unique challenges in terms of damage detection and monitoring due to their anisotropic nature and susceptibility to invisible damage.

The review discusses various NDE techniques that have been adapted and developed to inspect aerospace structures effectively. These include visual inspection, radiography, MPI, ECT, and UT. However, the limitations of these methods in providing continuous real-time monitoring of composite material utilized for aircraft structure have led to the advancement of SHM techniques.

The study reviews several types of SHM sensors, including fiber-optic sensors (interferometric, distributed, and grating-based), piezoelectric sensors (active and passive), and piezoresistive self-sensing systems. Fiber-optic sensors are noted for their high sensitivity and multiplexing capability, making them suitable for distributed sensing applications. Piezoelectric sensors are effective for both local and global damage detection, while piezoresistive self-sensing systems offer a promising approach by integrating sensing capabilities directly into the composite material.

Challenges in implementing SHM systems are identified, such as ensuring sensor durability in harsh environments, compensating for temperature variations, processing and analyzing

**ADVANCED
SCIENCE NEWS**

www.advancedsciencenews.com

**ADVANCED
ENGINEERING
MATERIALS**

www.aem-journal.com

large volumes of data, and integrating sensors with existing aircraft systems. The review suggests solutions such as protective coatings for sensors, advanced data processing algorithms, and modular system design to address these challenges.

In conclusion, the review underscores the importance of continuous research and development in SHM sensor technology for aerospace composite structures. The findings indicate that while significant progress has been made in the development of various SHM sensors and techniques, there is still a need for further innovation to improve sensor durability, enhance data processing capabilities, and ensure seamless integration with aircraft systems. As the aerospace industry continues to evolve, the effective implementation of SHM systems will be crucial for maintaining the structural integrity of composite materials and ensuring the safety of aerospace operations.

Acknowledgements

Conflict of Interest

The authors declare no conflict of interest.

Author Contributions

Raphael Olabanji Ogunleye: Conceptualization (lead); Data curation (lead); Formal analysis (lead); Investigation (lead); Methodology (lead); Validation (lead); Visualization (lead); Writing—original draft (lead); Writing—review & editing (lead). **Soňa Rusnáková**: Conceptualization (supporting); Funding acquisition (lead); Investigation (supporting); Methodology (supporting); Resources (lead); Supervision (lead); Validation (supporting); Visualization (supporting); Writing—original draft (supporting); Writing—review & editing (supporting). **Jakub Javořík**: Conceptualization (supporting); Data curation (supporting); Formal analysis (supporting); Funding acquisition (supporting); Investigation (supporting); Methodology (supporting); Project administration (supporting); Resources (supporting); Software (lead); Supervision (supporting); Validation (supporting). **Milan Žaludek**: Data curation (supporting); Formal analysis (supporting); Investigation (supporting); Methodology (supporting); Resources (supporting); Validation (supporting); Visualization (supporting). **Barbora Kotlánová**: Conceptualization (supporting); Funding acquisition (supporting); Project administration (supporting); Resources (supporting); Software (supporting); Writing—review & editing (supporting).

Keywords

[1] J. Zhang, G. Lin, U. Vaidya, H. Wang, *Composites, Part B* **2023**, *250*, 110463.

[2] S. Li, X. Yue, Q. Li, H. Peng, B. Dong, T. Liu, H. Yang, J. Fan, S. Shu, F. Qiu, Q. Jiang, *J. Mater. Res. Technol.* **2023**, *27*, 944.

[3] F. Khan, N. Hossain, J. J. Mim, S. M. Rahman, M. J. Iqbal, M. Billah, M. A. Chowdhury, *J. Eng. Res.* **2024**, https://doi.org/10.1016/j.jer.2024.02.017.

[4] S. Maiti, M. R. Islam, M. A. Uddin, S. Afroj, S. J. Eichhorn, N. Karim, *Adv. Sustainable Syst.* **2022**, *6*, 2200258.

[5] S. Siengchin, *Def. Technol.* **2023**, *24*, 1.

[6] X. Liu, C. Bai, X. Xi, S. Zhou, X. Zhang, X. Li, Y. Ren, J. Yang, X. Yang, *Prog. Aerosp. Sci.* **2024**, *148*, 101002.

[7] A. Y. Boroujeni, M. Tehrani, A. J. Nelson, M. Al-Haik, *Composites, Part B* **2014**, *66*, 475.

[8] Z. Zhou, Z. Cui, J. Liu, T. Kundu, *Eng. Fract. Mech.* **2023**, *277*, 108995.

[9] R. Barreira-Pinto, R. Carneiro, M. Miranda, R. M. Guedes, *Materials* **2023**, *16*, 3913.

[10] K. G. Andersen, G. Jombo, S. O. Ismail, Y. K. Chen, H. N. Dhakal, Y. Zhang, in *Energy and Sustainable Futures, Springer Proc. in Energy*, Springer, Cham, Germany **2021**, pp. 275–282.

[11] Z. Yang, C. Pei, H. Yan, L. Long, *Mater. Des. Process. Commun.* **2020**, *2*, https://doi.org/10.1002/mdp2.129.

[12] D. J. Munk, D. J. Auld, G. P. Steven, G. A. Vio, *Struct. Multidiscip. Optim.* **2019**, *60*, 1245.

[13] O. Ahmed, X. Wang, M.-V. Tran, M.-Z. Ismadi, *Composites, Part B* **2021**, *223*, 109136.

[14] R. Fuentes, E. J. Cross, P. A. Gardner, L. A. Bull, T. J. Rogers, R. J. Barthorpe, H. Shi, N. Dervilis, C. R. Farrar, K. Worden, *Handbook of Experimental Structural Dynamics*, Springer New York, New York, NY **2022**, pp. 989–1061.

[15] M. M. Azad, S. Kim, Y. Bin Cheon, H. S. Kim, *Adv. Compos. Mater.* **2024**, *33*, 162.

[16] M. Majumder, T. K. Gangopadhyay, A. K. Chakraborty, K. Dasgupta, D. K. Bhattacharya, *Sens. Actuators, A* **2008**, *147*, 150.

[17] K. Diamanti, C. Soutis, *Prog. Aerosp. Sci.* **2010**, *46*, 342.

[18] D.-Z. Dang, Y.-W. Wang, Y.-Q. Ni, *Constr. Build. Mater.* **2024**, *411*, 134728.

[19] R. K. Langat, E. De Luycker, A. Cantarel, M. Rakotondrabe, *Micromachines* **2024**, *15*, 274.

[20] P. Russo, V. Vespini, S. Coppola, F. Graziano, P. Ferraro, S. Grilli, M. Rippa, E. Stella, M. Nitti, V. Renò, G. Del Prete, V. Dentico, N. Gallo, V. Memmolo, E. Monaco, F. Ricci, in *Behavior and Mechanics of Multifunctional Materials XVIII* (Eds: A. Wissa, M. Gutierrez Soto, R. W. Mailen), SPIE, Bellingham **2024**, p. 3.

[21] R. H. Bossi, G. E. Georgeson, in *Polymer Composites in the Aerospace Industry*, Vol. 2 (Eds: P. Irving, C. Soutis), Woodhead Publishing, Sawston **2020**, Ch. 16.

[22] K. Sapountzi, *MSc Thesis*, University of Bristol **2019**.

[23] J. E. See, C. G. Drury, A. Speed, A. Williams, N. Khalandi, *Proc. Hum. Factors Ergon. Soc. Annu. Meet.* **2017**, *61*, 262.

[24] S. Zhong, W. Nsengiyumva, *Nondestructive Testing and Evaluation of Fiber-Reinforced Composite Structures*, Springer Nature Singapore, Singapore **2022**.

[25] Ö. Ulus, F. E. Davarcı, E. E. Gültekin, *Int. J. Aeronaut. Astronaut.* **2024**, *5*, 10.

[26] I. Jandejsek, J. Jakubek, M. Jakubek, P. Prucha, F. Krejci, P. Soukup, D. Turecek, D. Vavrik, J. Zemlicka, *J. Instrum.* **2014**, *9*, 1.

[27] E. Dilonardo, M. Nacucchi, F. De Pascalis, M. Zarrelli, C. Giannini, *Compos. Sci. Technol.* **2020**, *192*, 108093.

[28] A. I. Sacarea, G. Oancea, L. Parv, *Processes* **2021**, *9*, 1067.

[29] J. Jodhani, A. Handa, A. Gautam, . Ashwni, R. Rana, *Mater. Today Proc.* **2023**, *78*, 627.

[30] K. Bin Ali, A. N. Abdalla, D. Rifai, M. A. Faraj, *IET Circuits Devices Syst.* **2017**, *11*, 338.

**ADVANCED
SCIENCE NEWS**

www.advancedsciencenews.com

**ADVANCED
ENGINEERING
MATERIALS**

www.aem-journal.com

[31] C. Li, W. He, X. Nie, X. Wei, H. Guo, X. Wu, H. Xu, T. Zhang, X. Liu, *AIP Adv.* **2021**, *11*, 125227.

[32] M. Sreejith, R. S. Rajeev, in *Fiber Reinforced Composites Constituents, Compatibility, Perspectives, and Applications*, Vol. *1* (Eds: K. Joseph, K. Oksman, G. George, R. Wilson, S. Appukuttan), Woodhead Publishing, Sawston **2021**, Ch. 25.

[33] M. Bhong, T. K. H. Khan, B. Devade, B. Vijay Krishna, S. Sura, H. K. Eftikhaar, H. Pal Thethi, N. Gupta, *Mater. Today Proc.* **2023**, https://doi.org/10.1016/j.matpr.2023.10.026.

[34] J. Y. Choi, J. H. Jeon, J. H. Lyu, J. Park, G. Y. Kim, S. Y. Chey, Y.-J. Quan, B. Bhandari, B. G. Prusty, S.-H. Ahn, *Int. J. Precis. Eng. Manuf.-Green Technol.* **2023**, *10*, 269.

[35] T. Huang, M. Bobyr, *J. Compos. Sci.* **2023**, *7*, 468.

[36] S. Zhang, B. Ducharne, S. Takeda, G. Sebald, T. Uchimoto, *J. Magn. Magn. Mater.* **2021**, *531*, 167971.

[37] M. E. Ibrahim, *Composites, Part A* **2014**, *64*, 36.

[38] B. Wang, S. Zhong, T.-L. Lee, K. S. Fancey, J. Mi, *Adv. Mech. Eng.* **2020**, *12*, 168781402091376.

[39] S. M. O. Tavares, P. M. S. T. de Castro, *Damage Tolerance of Metallic Aircraft Structures*, Springer International Publishing, Cham **2019**.

[40] W. Wu, S. Cantero-Chinchilla, D. Prescott, R. Remenyte-Prescott, M. Chiachío, *Reliab. Eng. Syst. Saf.* **2024**, *250*, 110267.

[41] M. Memari, P. Shakya, M. Shekaramiz, A. C. Seibi, M. A. S. Masoum, *IEEE Access* **2024**, *12*, 33236.

[42] M. Javaid, A. Haleem, R. P. Singh, S. Rab, R. Suman, *Sens. Int.* **2021**, *2*, 100110.

[43] M. A. Musthaq, H. N. Dhakal, Z. Zhang, A. Barouni, R. Zahari, *Polymers* **2023**, *15*, 1229.

[44] G. Ólafsson, R. Tighe, S. Boyd, J. Dulieu-Barton, *Struct. Health Monit.* **2021**, *20*, 3406.

[45] A. Hornig, R. Frohberg, T. Bätzel, M. Gude, N. Modler, *Smart Mater. Struct.* **2022**, *31*, 095007.

[46] T. Siwowski, M. Rajchel, T. Howiacki, R. Sieńko, Ł. Bednarski, *Eng. Struct.* **2021**, *246*, 113057.

[47] K. I. Tserpes, V. Karachalios, I. Giannopoulos, V. Prentzias, R. Ruzek, *Compos. Struct.* **2014**, *107*, 726.

[48] R. Di Sante, L. Donati, *Measurement* **2013**, *46*, 2118.

[49] V. Ivanov, L. Longoni, M. Ferrario, M. Brunero, D. Arosio, M. Papini, *Eng. Geol.* **2021**, *288*, 106128.

[50] K. Peters, D. Inaudi, in *Sensor Technologies for Civil Infrastructures*, Vol. *1* (Eds: J. P. Lynch, M. L. Wang), Woodhead Publishing, Sawston **2022**, Ch. 5.

[51] S. Komatsuzaki, S. Kojima, A. Hongo, N. Takeda, T. Sakurai, in *Proc. Sensor Systems and Networks: Phenomena, Technology, and Applications for NDE and Health Monitoring* (Ed: K. J. Peters), SPIE, Bellingham **2007**, p. 6530.

[52] S. N. Khonina, N. L. Kazanskiy, M. A. Butt, *Biosensors* **2023**, *13*, 835.

[53] C. K. Y. Leung, Z. Yang, Y. Xu, P. Tong, S. K. L. Lee, *Sens. Actuators, A* **2005**, *119*, 336.

[54] Y. J. Rao, D. A. Jackson, *Optical Fiber Sensor Technology*, Springer US, Boston, MA **2000**, pp. 167–191.

[55] G. Zhou, L. M. Sim, *Opt. Lasers Eng.* **2009**, *47*, 1063.

[56] H. F. Taylor, in *Fiber Optic Sensors*, Vol. *2* (Eds: S. Yin, P. B. Ruffin, F. T. S. Yu), CRC Press, Boca Raton **2017**, Ch. 2.

[57] W.-H. Tsai, C.-J. Lin, *J. Lightwave Technol.* **2001**, *19*, 682.

[58] Y.-J. Rao, *Opt. Fiber Technol.* **2006**, *12*, 227.

[59] Z. Wu, Y. Guo, J. Zhou, X. Fan, Z. Pei, Q. Zhang, *IEEE Trans. Dielectr. Electr. Insul.* **2024**, *31*, 591.

[60] J. Johny, S. Amos, R. Prabhu, *Sensors* **2021**, *21*, 6047.

[61] M. Á. Ramírez-Hernández, M. Alonso-Murias, D. Monzón-Hernández, *J. Lightwave Technol.* **2024**, *42*, 3430.

[62] D. Yang, Y. Liu, Y. Wang, T. Zhang, M. Shao, D. Yu, H. Fu, Z. Jia, *Opt. Laser Technol.* **2020**, *126*, 106112.

[63] K. M. Tripathi, F. Vincent, M. Castro, J. F. Feller, *Nanocomposites* **2016**, *2*, 125.

[64] J. R. Carvalho, *MSc*, University of Johannesburg, **2022**.

[65] J. Leng, A. Asundi, *Sens. Actuators, A* **2003**, *103*, 330.

[66] J. Yu, Q. Bian, Y. Tong, Z. Zhu, *J. Phys.: Conf. Ser.* **2021**, *2005*, 012047.

[67] J. Yin, T. Liu, J. Jiang, K. Liu, S. Wang, F. Wu, Z. Ding, *Opt. Lett.* **2013**, *38*, 3751.

[68] J. Guillen Bonilla, A. Guillen Bonilla, V. Rodríguez Betancourtt, H. Guillen Bonilla, A. Casillas Zamora, *Sensors* **2017**, *17*, 859.

[69] Y. Ou, C. Zhou, A. Zheng, C. Cheng, D. Fan, J. Yin, H. Tian, M. Li, Y. Lu, *Appl. Opt.* **2014**, *53*, 8358.

[70] Y. Zhang, Y. Jiang, S. Yang, D. Zhang, *Opt. Express* **2024**, *32*, 14826.

[71] M. Barile, L. Lecce, M. Iannone, S. Pappadà, P. Roberti, *Revolutionizing Aircraft Materials and Processes*, Springer International Publishing, Cham **2020**, pp. 87–114.

[72] H. Wijaya, P. Rajeev, E. Gad, *Opt. Fiber Technol.* **2021**, *64*, 102577.

[73] A. Masoudi, M. Belal, T. P. Newson, *Meas. Sci. Technol.* **2013**, *24*, 085204.

[74] Y. Gong, O. L. C. Michael, J. Hao, V. Paulose, *Opt. Commun.* **2007**, *280*, 91.

[75] X. Feng, J. Zhou, C. Sun, X. Zhang, F. Ansari, *J. Eng. Mech.* **2013**, *139*, 1797.

[76] R. Zinsou, X. Liu, Y. Wang, J. Zhang, Y. Wang, B. Jin, *Sensors* **2019**, *19*, 1709.

[77] A. Datta, M. J. Augustin, K. M. Gaddikeri, S. R. Viswamurthy, N. Gupta, R. Sundaram, *Opt. Fiber Technol.* **2021**, *66*, 102651.

[78] P. F. Díaz-Maroto, N. Gutiérrez, A. Fernández, R. Fernández, F. Lasagni, J. A. Güemes, in *8th European Workshop On Structural Health Monitoring, E-Journal Of Nondestructive Testing*, Bilbao, Spain **2016**, pp. 1–9.

[79] A. Hong, L. Peng, S. Guo, Z. Liu, in *Proc. of 2012 Int. Conf. Measurement, Information and Control*, IEEE, Piscataway, NJ **2012**, pp. 668–672.

[80] Y. Zhan, M. Han, Z. Wang, L. Xu, Z. Song, A. Lu, X. Guo, W. Deng, S. Huang, *Optik* **2021**, *248*, 168113.

[81] F. Wang, W. Zhan, X. Zhang, Y. Lu, *J. Lightwave Technol.* **2013**, *31*, 3663.

[82] A. S. K. Almoosa, A. E. Hamzah, M. S. D. Zan, M. F. Ibrahim, N. Arsad, M. M. Elgaud, *Opt. Fiber Technol.* **2022**, *70*, 102860.

[83] S. Jothibasu, Y. Du, S. Anandan, G. S. Dhaliwal, R. E. Gerald, S. E. Watkins, K. Chandrashekhara, J. Huang, *Opt. Eng.* **2019**, *58*, 1.

[84] H. Lu, X. Gu, in *Opto-Mechanical Fiber Optic Sensors*, Vol. *1* (Ed: H. Alemohammad), Elsevier, Amsterdam **2018**, Ch. 4.

[85] W. Jin, T. K. Y. Lee, S. L. Ho, H. L. Ho, K. T. Lau, L. M. Zhou, Y. Zhou, in *Guided Wave Optical Components and Devices*, Vol. *1* (Ed: B. P. Pal), Elsevier, Amsterdam **2006**, Ch. 25.

[86] B. da Silva Falcão, A. Giwelli, M. Nogueira Kiewiet, S. Banks, G. Yabesh, L. Esteban, L. Kiewiet, N. Yekeen, Y. Kovalyshen, L. Monmusson, A. Al-Yaseri, A. Keshavarz, S. Iglauer, *Heliyon* **2023**, *9*, e18652.

[87] D. Kinet, P. Mégret, K. Goossen, L. Qiu, D. Heider, C. Caucheteur, *Sensors* **2014**, *14*, 7394.

[88] J. Huang, Z. Zhou, X. Wen, D. Zhang, *Measurement* **2013**, *46*, 1041.

[89] A. Venketeswaran, N. Lalam, J. Wuenschell, P. R. Ohodnicki, M. Badar, K. P. Chen, P. Lu, Y. Duan, B. Chorpening, M. Buric, *Adv. Intell. Syst.* **2022**, *4*, 2100067.

[90] A. R. Upadhya, G. N. Dayananda, G. M. Kamalakannan, J. Ramaswamy Setty, J. Christopher Daniel, *Int. J. Aerosp. Eng.* **2011**, *2011*, 1.

[91] G. C. Kahandawa, J. Epaarachchi, H. Wang, K. T. Lau, *Photonic Sens.* **2012**, *2*, 203.

[92] R. de Oliveira, S. Lavanchy, R. Chatton, D. Costantini, V. Michaud, R. Salathé, J.-A. E. Mânson, *Composites, Part A* **2008**, *39*, 1083.

[93] X. Yi, X. Chen, H. Fan, F. Shi, X. Cheng, J. Qian, *Opt. Express* **2020**, *28*, 9367.

[94] S. Jeong, S. Choi, J. Pan, *IET Sci., Meas. Technol.* **2020**, *14*, 41.

[95] X. Mao, X. Zhou, H. Ye, Y. Tan, Y. Luo, *Infrared Phys. Technol.* **2023**, *128*, 104490.

[96] B. Li, Z.-W. Tan, H. Zhang, P. P. Shum, D. J. Hu, L. J. Wong, *Opt. Lett.* **2023**, *48*, 2114.

[97] D. Tosi, *J. Sens.* **2017**, *2017*, 1.

[98] M. P. Fernández, L. A. Bulus Rossini, J. L. Cruz, M. V. Andrés, P. A. Costanzo Caso, *Opt. Express* **2019**, *27*, 36815.

[99] C. Wang, J. Yao, *J. Lightwave Technol.* **2011**, *29*, 2927.

[100] Y. Li, B. Lu, L. Ren, H. Chen, Y. Qiu, B. Mao, P. Zhou, C. Zhao, X. Dong, *Opt. Fiber Technol.* **2019**, *48*, 207.

[101] E. S. Kocaman, C. J. Keulen, E. Akay, M. Yildiz, H. S. Turkmen, A. Suleman, *Sci. Eng. Compos. Mater.* **2016**, *23*, 711.

[102] H. Rocha, C. Semprimoschnig, J. P. Nunes, *CEAS Space J.* **2021**, *13*, 353.

[103] R. Liu, D. Liang, A. Asundi, *Measurement* **2013**, *46*, 3440.

[104] V. S. Kathavate, K. E. Prasad, M. S. R. N. Kiran, Y. Zhu, *J. Appl. Phys.* **2022**, *132*, 121103.

[105] S. S. Dani, A. Tripathy, N. R. Alluri, S. Balasubramaniam, A. Ramadoss, *Mater. Adv.* **2022**, *3*, 8886.

[106] J. Wen, W. Wu, Z. Xie, J. Wu, *Macromol. Mater. Eng.* **2023**, *308*, 2300101.

[107] F. Sha, D. Xu, X. Cheng, S. Huang, *Res. Nondestr. Eval.* **2021**, *32*, 88.

[108] B. Chen, H. Li, W. Tian, C. Zhou, *J. Electron. Mater.* **2019**, *48*, 2916.

[109] L. Yuan, W. Fan, X. Yang, S. Ge, C. Xia, S. Y. Foong, R. K. Liew, S. Wang, Q. Van Le, S. S. Lam, *Compos. Commun.* **2021**, *25*, 100680.

[110] J. Tolvanen, J. Hannu, J. Juuti, H. Jantunen, *Electron. Mater. Lett.* **2018**, *14*, 113.

[111] Q. Feng, Y. Liang, *Earthquake Res. Adv.* **2023**, *3*, 100154.

[112] V. Giurgiutiu, *J. Phys. Conf. Ser.* **2011**, *305*, 012123.

[113] H. Mei, M. Haider, R. Joseph, A. Migot, V. Giurgiutiu, *Sensors* **2019**, *19*, 383.

[114] U. Meher, M. Rabius Sunny, *Mech. Syst. Signal Process.* **2024**, *220*, 111661.

[115] W. Ostachowicz, R. Soman, P. Malinowski, *Struct. Health Monit.* **2019**, *18*, 963.

[116] T. Wandowski, P. H. Malinowski, W. M. Ostachowicz, *Compos. Struct.* **2016**, *151*, 99.

[117] Y.-F. Su, G. Han, T. Nantung, N. Lu, *Constr. Build. Mater.* **2020**, *259*, 119848.

[118] P. E. C. Pereira, S. W. F. de Rezende, H. C. Fernandes, J. D. R. V. de Moura Junior, R. M. Finzi Neto, *J. Braz. Soc. Mech. Sci. Eng.* **2024**, *46*, 311.

[119] K. K. Maurya, A. Rawat, G. Jha, *Mater. Today Proc.* **2020**, *33*, 4993.

[120] J. Deng, X. Li, M. Zhu, K. Rashid, Q. Wang, *Constr. Build. Mater.* **2021**, *303*, 124431.

[121] R. Tawie, H. B. Park, J. Baek, W. S. Na, *Sensors* **2019**, *19*, 1000.

[122] P. Cao, S. Zhang, Z. Wang, K. Zhou, *Structures* **2023**, *50*, 1906.

[123] F. G. Baptista, J. V. Filho, D. J. Inman, *Struct. Health Monit.* **2012**, *11*, 173.

[124] S. da Silva, M. O. Yano, C. G. Gonsalez-Bueno, *J. Nondestr. Eval.* **2021**, *40*, 64.

[125] A. Lejeune, N. Hascoët, M. Rébillat, E. Monteiro, N. Mechbal, *Struct. Health Monit.* **2023**, *21*, 2200.

[126] N. Ismail, M. H. Zohari, C. K. Eddy, C. K. Nizwan, K. S. Lim, *J. Adv. Res. Appl. Sci. Eng. Technol.* **2024**, *42*, 38.

[127] M. Voß, A. Szewieczek, W. Hillger, T. Vallée, F. von Dungern, *Adv. Compos. Mater.* **2024**, *33*, 22.

[128] C.-D. Chen, Y.-J. Shen, P.-Y. Chou, P.-H. Wang, *Smart Mater. Struct.* **2024**, *33*, 045028.

[129] X. Zeng, B. Zhao, X. Liu, Y. Yu, J. Guo, X. Qing, *Mech. Syst. Signal Process.* **2023**, *184*, 109750.

[130] N. Zhang, M. Zhai, L. Zeng, L. Huang, J. Lin, *Compos. Struct.* **2023**, *307*, 116642.

[131] K. Balasubramaniam, S. Sikdar, D. Ziaja, M. Jurek, R. Soman, P. Malinowski, *Smart Mater. Struct.* **2023**, *32*, 035016.

[132] A. S. Purekar, D. J. Pines, *J. Intell. Mater. Syst. Struct.* **2010**, *21*, 995.

[133] V. Memmolo, E. Monaco, N. D. Boffa, L. Maio, F. Ricci, *Compos. Struct.* **2018**, *184*, 568.

[134] L. Capineri, A. Bulletti, *Sensors* **2021**, *21*, 2929.

[135] S. Masmoudi, A. El Mahi, S. Turki, *Appl. Acoust.* **2016**, *108*, 50.

[136] A. J. Brunner, *Appl. Sci.* **2021**, *11*, 11648.

[137] S. Sikdar, W. Ostachowicz, J. Pal, *Compos. Struct.* **2018**, *202*, 860.

[138] S. Masmoudi, A. El Mahi, R. El Guerjouma, *Composites, Part B* **2014**, *67*, 76.

[139] S. Masmoudi, A. El Mahi, S. Turki, R. El Guerjouma, in *Design and Modeling of Mechanical Systems*, Springer, Cham, Germany **2013**, pp. 307–314.

[140] S. Masmoudi, A. El Mahi, S. Turki, *Composites, Part B* **2015**, *80*, 307.

[141] S. Samborski, I. Korzec, *Adv. Sci. Technol. Res. J.* **2023**, *17*, 210.

[142] N. S. Ghadarah, D. Ayre, *Compos. Sci. Technol.* **2024**, *247*, 110392.

[143] B. Bhandari, P. T. Maung, G. B. Prusty, *Sensors* **2024**, *24*, 3450.

[144] P. Shivashankar, S. Gopalakrishnan, *Smart Mater. Struct.* **2020**, *29*, 053001.

[145] P. Cawley, *Struct. Health Monit.* **2018**, *17*, 1225.

[146] W. J. Staszewski, S. Mahzan, R. Traynor, *Compos. Sci. Technol.* **2009**, *69*, 1678.

[147] A. S. Fiorillo, C. D. Critello, S. A. Pullano, *Sens. Actuators, A* **2018**, *281*, 156.

[148] Q. Xiang, H. Zhang, Z. Liu, Y. Zhao, H. Tan, *Chem. Eng. J.* **2024**, *480*, 147825.

[149] T. Seesaard, C. Wongchoosuk, *Micromachines* **2023**, *14*, 1638.

[150] J. Li, L. Fang, B. Sun, X. Li, S. H. Kang, *J. Electrochem. Soc.* **2020**, *167*, 037561.

[151] J. Wen, Z. Xia, F. Choy, *Composites, Part B* **2011**, *42*, 77.

[152] X. Wang, B. Cao, C. Vlachakis, A. Al-Tabbaa, S. K. Haigh, *Cem. Concr. Compos.* **2023**, *142*, 105187.

[153] P. Verma, J. Ubaid, K. M. Varadarajan, B. L. Wardle, S. Kumar, *ACS Appl. Mater. Interfaces* **2022**, *14*, 8361.

[154] V. Parvaneh, S. H. Khiabani, *Mech. Adv. Mater. Struct.* **2019**, *26*, 993.

[155] D. D. L. Chung, *J. Mater. Sci.* **2020**, *55*, 15367.

[156] D. Kannichankandy, P. M. Pataniya, S. Narayan, V. Patel, C. K. Sumesh, K. D. Patel, G. K. Solanki, V. M. Pathak, *Synth. Met.* **2021**, *273*, 116697.

[157] C. Xu, H. Lu, Z. Liu, N. Luo, A. Wei, *J. Mater. Sci.: Mater. Electron.* **2023**, *34*, 906.

[158] C. C. Bowland, N. A. Nguyen, A. K. Naskar, *ACS Appl. Mater. Interfaces* **2018**, *10*, 26576.

[159] G. Selleri, M. E. Gino, T. M. Brugo, R. D'Annibale, J. Tabucol, M. L. Focarete, R. Carloni, D. Fabiani, A. Zucchelli, *Mater. Des.* **2022**, *219*, 110787.

[160] V. Kostopoulos, A. Vavouliotis, P. Karapappas, P. Tsotra, A. Paipetis, *J. Intell. Mater. Syst. Struct.* **2009**, *20*, 1025.

[161] L. Tzounis, M. Zappalorto, F. Panozzo, K. Tsirka, L. Maragoni, A. S. Paipetis, M. Quaresimin, *Composites, Part B* **2019**, *169*, 37.

[162] S. Luo, W. Obitayo, T. Liu, *Carbon* **2014**, *76*, 321.

[163] S. Luo, T. Liu, *ACS Appl. Mater. Interfaces* **2014**, *6*, 9314.

[164] J. Wang, J. Suo, Z. Song, W. J. Li, Z. Wang, *Int. J. Extreme Manuf.* **2023**, *5*, 032013.

[165] M. H. Islam, S. Afroj, M. A. Uddin, D. V. Andreeva, K. S. Novoselov, N. Karim, *Adv. Funct. Mater.* **2022**, *32*, 2205723.

[166] J.-M. Park, D.-S. Kim, J.-R. Lee, T.-W. Kim, *Mater. Sci. Eng., C* **2003**, *23*, 971.

[167] D. Mi, Z. Zhao, H. Bai, *Polymers* **2023**, *15*, 2370.

[168] B. N. Duc, Y. Son, *Compos. Commun.* **2020**, *21*, 100420.

[169] Y. Wu, X. Cheng, S. Chen, B. Qu, R. Wang, D. Zhuo, L. Wu, *Mater. Des.* **2021**, *202*, 109535.

[170] G. Sapra, P. Kumar, N. Kumar, R. Vig, M. Sharma, *J. Mater. Sci.: Mater. Electron.* **2018**, *29*, 19264.

[171] S. Datta, R. K. Neerukatti, A. Chattopadhyay, *Carbon* **2018**, *139*, 353.

[172] A. S. Paipetis, V. Kostopoulos, in *Carbon Nanotube Enhanced Aerospace Composite Materials*, Springer, Cham, Germany **2013**, pp. 1–20.

[173] B. R. Loyola, V. La Saponara, K. J. Loh, *J. Mater. Sci.* **2010**, *45*, 6786.

[174] I. W. Nam, S. M. Park, H. K. Lee, L. Zheng, *Compos. Struct.* **2017**, *178*, 1.

[175] R. G. Qhobosheane, M. M. Rabby, V. Vadlamudi, K. Reifsnider, R. Raihan, *Ceramics* **2022**, *5*, 253.

[176] M. A. Rahman, H. Taheri, F. Dababneh, S. S. Karganroudi, S. Arhamnamazi, *Mech. Syst. Signal Process.* **2024**, *208*, 110983.

[177] Y. Li, Z. Sharif-Khodaei, *Mech. Syst. Signal Process.* **2024**, *208*, 110954.

[178] X. Qing, W. Li, Y. Wang, H. Sun, *Sensors* **2019**, *19*, 545.

[179] S. Mustapha, Y. Lu, C.-T. Ng, P. Malinowski, *Vibration* **2021**, *4*, 551.

[180] M. AlHamaydeh, N. Ghazal Aswad, *Pract. Period. Struct. Des. Constr.* **2022**, *27*, 03122004.

[181] X. Huang, S. M. Haneef, M. Davies, D. A. Moseley, B. M. Ludbrook, E. E. Salazar, A. N. Chalmers, R. A. Badcock, *Opt. Fiber Technol.* **2023**, *80*, 103419.

[182] M. González-Gallego, F. Terroba Ramírez, J. L. Martínez-Vicente, M. González del Val, J. J. López-Cela, M. Frövel, *Polymers* **2024**, *16*, 1223.

[183] S. Goossens, B. De Pauw, T. Geernaert, M. S. Salmanpour, Z. Sharif Khodaei, E. Karachalios, D. Saenz-Castillo, H. Thienpont, F. Berghmans, *Smart Mater. Struct.* **2019**, *28*, 065008.

[184] X. Qing, Y. Liao, Y. Wang, B. Chen, F. Zhang, Y. Wang, *Int. J. Smart Nano Mater.* **2022**, *13*, 167.

[185] A. G. Mohapatra, A. Khanna, D. Gupta, M. Mohanty, V. H. C. de Albuquerque, *Comput. Intell.* **2022**, *38*, 747.

[186] O. Ejiohuo, *NanoTrends* **2023**, *4*, 100025.

[187] M. S. Kumar, A. J. Rani, *Comput. Electr. Eng.* **2018**, *72*, 169.

[188] Y. Wang, L. Qiu, Q. Xu, L. Shi, *Chin. J. Aeronaut.* **2024**, *37*, 153.

[189] M. Strohmeier, G. Tresoldi, L. Granger, V. Lenders, in *Proc. 15th Workshop on Cyber Security Experimentation and Test*, ACM, New York, NY **2022**, pp. 10–18.

[190] J. Horrell, Imperial College Press, London **2024**, https://www.imperial.ac.uk/news/252273/lightweight-tech-game-changer-sustainable-aircraft-heath/.

[191] F. Siddiqui, A. Ahlbrecht, R. Khan, S. Y. Tasdemir, H. Hui, B. Sonigara, S. Sezer, K. McLaughlin, W. Zaeske, U. Durak, in *2023 IEEE/AIAA 42nd Digital Avionics Systems Conf. (DASC)*, IEEE, Piscataway, NJ **2023**, pp. 1–8.

[192] L. Kuan, L. Aijun, W. Tianbo, L. Linxiao, W. Jianyuan, in *Proc. 5th China Aeronautical Science and Technology Conf.*, Springer, Singapore **2022**, pp. 951–962.

[193] P. Wilde, C. Draper, in *48th AIAA Aerospace Sciences Meeting Including the New Horizons Forum and Aerospace Exposition*, American Institute of Aeronautics and Astronautics, Reston, Virigina **2010**.

[194] A. B. Garcia, R. F. Babiceanu, R. Seker, in *2021 Integrated Communications Navigation and Surveillance Conf. (ICNS)*, IEEE, Piscataway, NJ **2021**, pp. 1–8.

[195] J. Aust, A. Mitrovic, D. Pons, *Aerospace* **2021**, *8*, 313.

[196] A. Yunker, R. Kettimuthu, Z. Kral, in *ASME 2024 Aerospace Structures, Structural Dynamics, and Materials Conf.*, American Society of Mechanical Engineers, Renton **2024**.

[197] D. Linardatos, V. Koukou, N. Martini, A. Konstantinidis, A. Bakas, G. Fountos, I. Valais, C. Michail, *Materials* **2021**, *14*, 888.

[198] A. Sardellitti, F. Milano, M. Laracca, S. Ventre, L. Ferrigno, A. Tamburrino, *IEEE Trans. Instrum. Meas.* **2023**, *72*, 1.

[199] J. Ai, Q. Zhou, X. Zhang, S. Li, B. Long, L. Bai, *Appl. Sci.* **2023**, *13*, 4541.

[200] Y. Liu, J. Yin, Y. Tian, X. Fan, *Sensors* **2019**, *19*, 2171.

[201] N. Lalam, H. Bhatta, M. Buric, R. Wright, in *Photonic Instrumentation Engineering XI* (Eds: Y. Soskind, L. E. Busse), SPIE, Bellingham **2024**, p. 32.

[202] X. Cheng, X. Cao, Z. Wu, Z. Ying, D. Camilleri, X. Hu, *Adv. Eng. Mater.* **2023**, *25*, 2300341.

[203] J. A. Rodríguez-González, C. Rubio-González, *Polym. Compos.* **2022**, *43*, 3276.

[204] Z. Zhang, H. Wei, Y. Liu, J. Leng, *Struct. Health Monit.* **2015**, *14*, 127.

[205] A. Can-Ortiz, A. I. Oliva-Avilés, F. Gamboa, A. May-Pat, C. Velasco-Santos, F. Avilés, *J. Mater. Sci.* **2019**, *54*, 2205.

[206] A. Miliou, *Photonics* **2021**, *8*, 265.

[207] C. Sbarufatti, A. Manes, M. Giglio, *Struct. Control Health Monit.* **2014**, *21*, 1057.

[208] Y. Marin, T. Nannipieri, C. J. Oton, F. Di Pasquale, in *Proc. 25th Int. Conf. on Optical Fiber Sensors* (Eds: Y. Chung, W. Jin, B. Lee, J. Canning, K. Nakamura, L. Yuan), SPIE, Bellingham **2017**, p. 10323.

[209] P. Jiao, K.-J. I. Egbe, Y. Xie, A. Matin Nazar, A. H. Alavi, *Sensors* **2020**, *20*, 3730.

[210] S. Nauman, *Eng* **2021**, *2*, 197.
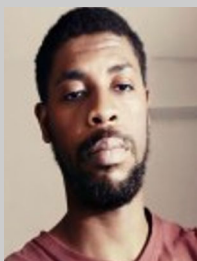
Raphael Olabanji Ogunleye holds a bachelor's and a master's degree in chemical engineering. He is currently a doctoral researcher at the Department of Production Engineering, Tomas Bata University in Zlin, Czech Republic. His research interest includes process engineering, polymer engineering, material engineering, FEM simulation, analysis, and design.
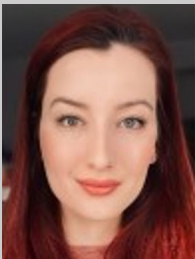
Soňa Rusnáková is an associate professor and lecturer at the Department of Production Engineering, Tomas Bata University in Zlin, Czech Republic. Her research interest include mechanical engineering and material science and engineering.

Jakub Javořík is an associate professor and lecturer at the Department of Production Engineering, Tomas Bata University in Zlin, Czech Republic. His research interest include mechanical engineering, material engineering, FEM analysis, and mechanic of polymers.

Milan Žaludek is an assistant professor and lecturer at the Department of Production Engineering, Tomas Bata University in Zlin, Czech Republic. His research interest include mechanical engineering and material testing and characterisation.

Barbora Kotlánová holds a bachelor's and a master's degree in production engineering and currently a doctoral researcher in the Department of Production Engineering, Tomas Bata University in Zlin, Czech Republic. Her research interest include mechanical engineering, material science and engineering, FEM analysis, and mechanics of polymers.